Available online at www.sciencedirect.com
SCIENCE DIRECT®
Progress in Retinal and Eye Research 24 (2005) 217–240
Progress in RETINAL AND EYE RESEARCH
www.elsevier.com/locate/prer

Understanding mechanisms of pressure-induced optic nerve damage

John C. Morrison*, Elaine C. Johnson, William Cepurna, Lijun Jia

Kenneth C. Swan Ocular Neurobiology Laboratory, Casey Eye Institute, Oregon Health and Sciences University, 3375 S.W Terwilliger Blvd., Portland, OR 97239, USA

Abstract

Patients with glaucoma can suffer progressive vision loss, even in the face of what appears to be excellent intraocular pressure (IOP) control. Some of this may be secondary to non-pressure-related (pressure-independent) factors. However, it is likely that chronically elevated IOP produces progressive changes in the optic nerve head, the retina, or both that alter susceptibility of remaining optic nerve fibers to IOP. In order to understand the nature of these progressive changes, relevant, cost-effective animal models are necessary. Several rat models are now used to produce chronic, elevated IOP, and methods exist for measuring the resulting IOP and determining the extent of the damage this causes to the retina and optic nerve. A comparison of damage, pressure and duration shows that these models are not necessarily equivalent.

These tools are beginning to uncover clear evidence that elevated IOP produces progressive changes in the optic nerve head and retina. In the optic nerve head, these include axonal and non-axonal effects, the latter pointing to involvement of extracellular matrix and astrocyte responses. In the retina, retinal ganglion cells appear to undergo changes in neurotrophin response as well as morphologic changes prior to actual cell death. These, and other, as yet uncovered, abnormalities in the optic nerve head and retina may influence relative susceptibility to IOP and explain progressive optic nerve damage and visual field loss, in spite of apparent, clinically adequate IOP control. Ultimately, this knowledge may lead to the development of new treatments designed to preserve vision in these difficult patients.

Keywords: Glaucoma; Intraocular pressure; Optic nerve damage; Glaucomatous optic neuropathy; Animal models

Contents

*Corresponding author. Tel.: +1-503-494-3038; +1-503-494-3075.
E-mail address: morrisoj@ohsu.edu (J.C. Morrison).

1350-9462/$ - see front matter © 2004 Elsevier Ltd. All rights reserved.
doi:10.1016/j.preteyeres.2004.08.003

1. Introduction

1.1. Clinical characteristics of glaucomatous optic nerve damage

Clinically, glaucoma is characterized by "cupping" of the optic nerve head and a specific pattern of visual field loss. Cupping appears to result from a combination of loss of retinal ganglion cell (RGC) axons along with the collapse and posterior bowing of the connective tissue sheets of the lamina cribrosa. In eyes with advanced damage, the cup extends laterally and beneath the scleral edge, producing undermining. In many patients, these physical changes are most pronounced in the superior and inferior poles of the optic nerve head, leading to vertical enlargement of the cup and focal erosion, or notching, of the neural rim.

Visual field loss in glaucoma results from dropout of RGC and their axons. Careful clinical-histopathologic studies have correlated visual field loss with optic nerve atrophy (Quigley et al., 1981; Quigley and Green, 1979), loss of RGC axons (Quigley et al., 1988; Quigley and Green, 1979) and with reduced numbers of RGC (Kerrigan-Baumrind et al., 2000; Quigley et al., 1989). Some, but not all, investigators have also noted changes in the outer retina (Nork et al., 2000; Quigley, 2001). The most characteristic visual field defect in glaucoma is the arcuate defect, or scotoma, emanating from the blind spot. These arcuate scotomas arch either above or below central fixation, and follow the pathways of the nerve fiber bundles as their axons converge from their RGC of origin on the superior and inferior poles of the optic nerve (Sommer et al., 1991; Tuulonen and Airaksinen, 1991). These fiber bundles do not anatomically cross a horizontal midline, which passes through the fovea. The resulting arcuate field defects also do not cross the midline, producing characteristic nasal "steps". Clinicopathologic studies of glaucomatous eyes support this superior:inferior predilection for injury, and document that axons of the superior and inferior optic nerve atrophy first, producing an "hour-glass" configuration of injury (Quigley and Green, 1979).

In spite of several analyses, only the structure of the optic nerve head has been found to correlate with this pattern of injury. In humans, the pores of the lamina cribrosa appear larger within the superior and inferior regions of the lamina cribrosa, along with thinner and less numerous connective tissue laminar beams (Quigley et al., 1981). The lamina cribrosa consists of multiple "plates" of connective tissue composed of several types of interstitial collagen, proteoglycans and elastin (Hernandez, 1992; Morrison et al., 1988, 1994). The plates are perforated by holes through which the optic nerve fiber bundles pass to form the optic nerve. This correlation of lamina cribrosa anatomy with apparent increased susceptibility of the superior and inferior optic disc in human glaucoma suggests strongly that the optic nerve head is a likely site of early injury in glaucoma.

Optic nerve damage, and vision loss, in chronic glaucoma is generally slow and progressive, usually occurring over years and decades. A region of the visual

field that is initially apparently normal will later develop a scotoma, without an apparent change in intraocular pressure (IOP), a well-recognized risk factor for glaucoma. Thus, susceptibility to IOP would appear to increase over time. As a clinical observation, Chandler and Grant emphasized years ago that patients with greater amounts of nerve damage and visual field loss appeared to suffer progressive visual loss at levels of IOP that would be tolerated by eyes with less damage. This observation, corroborated recently by the AGIS study (2000), suggests that there is something unique about the glaucomatous eye that renders the remaining optic nerve fibers more susceptible to IOP. We believe that understanding the nature of these changes will provide key information for understanding why many patients continue to progress despite apparently successful pressure lowering. It will also be important for developing specific treatments designed to reverse or stabilize these conditions and successfully preserve remaining nerve fibers and ensure their continued function.

Progressive susceptibility is most likely the result of unique features of the glaucomatous process. We believe that the most likely explanation lies in the occurrence of gradual changes at either the optic nerve head, within RGCs, or both. For instance, Quigley, studying glaucomatous optic nerve heads by scanning electron microscopy, found that the initial anatomic evidence of injury was posterior collapse of the anterior lamina cribrosa, primarily in the vertical poles of the optic nerve head (Quigley et al., 1981). This was followed later by more pronounced backwards bowing of the entire lamina cribrosa. Burgoyne has argued that such alterations represent a progressive failure of support for optic nerve fibers within the optic nerve head (Bellezza et al., 2003). There is currently little evidence for progressive retinal changes in human glaucoma.

Lack of non-invasive methods for assaying cellular function in humans has severely limited our understanding of how cells in the optic nerve head and retina respond in human glaucoma. Because of this, we currently rely heavily on relevant animal models, with which it will be possible to study these cellular responses.

1.2. Use of animal models for understanding glaucomatous optic nerve damage

The most widely developed animal models of glaucoma rely on experimentally elevating IOP, a well-known risk factor for glaucoma. Although it must be acknowledged that many glaucoma patients still demonstrate visual field progression in spite of clinically acceptable IOP reduction, this is the only glaucoma risk factor against which all current glaucoma therapy is directed. Furthermore, several recent large clinical studies have confirmed that aggressively treating IOP is beneficial in both normal pressure and primary open angle glaucoma (Drance, 1999; Leske et al., 2003), as well as ocular hypertension (Kass et al., 2002). It is best to consider these models as models of pressure-induced optic nerve damage, rather than strictly glaucoma models. However, it is reasonable to expect that understanding the mechanisms by which elevated IOP causes optic nerve damage will be highly relevant to our understanding of optic nerve damage in glaucoma and useful for developing and testing specific therapies to preserve vision in this large number of glaucoma patients.

Models of chronically elevated IOP can either be naturally occurring and sporadic, or experimentally induced (Morrison et al., 1999a, 1998). The former carry the advantage of a generally slow onset and buildup of IOP. In addition, these animals do not undergo experimental manipulations that could induce responses that might be mistakenly attributed to a response to the pressure. Disadvantages of spontaneous models are that they are generally bilateral, and thus lack a built-in control. In addition, as the timing of the IOP increase is somewhat unpredictable, careful studies of early events in the damage process may be difficult to determine.

Experimental models of pressure-induced optic nerve damage address both of these drawbacks. Because the pressure elevation is unilateral, the fellow eye is available as a control for the effects of inter-animal variability. In addition, the onset of the pressure elevation usually occurs at a relatively predictable time following the experimental manipulation. This allows the investigator to understand the sequential events of optic nerve and retina damage from elevated IOP.

The purpose of this paper is to review our current understanding of the mechanisms of pressure-induced optic nerve damage as gleaned from work with the available animal models of experimentally induced pressure elevation. This will include a discussion of currently available monkey and rat models. Attention will then be paid to cellular responses occurring within the ONH and RGC that may help to explain the pattern of pressure-induced injury and the progressive nature of vision loss in this disease.

2. Animal models of experimental pressure-induced optic nerve damage

Three major challenges must be addressed with any model of experimentally induced optic nerve damage. These include developing methods for measuring IOP, assessing optic nerve damage and creating chronic IOP elevation. Pressure measurements must accurately reflect

the level of pressure to which the ONH and retina are exposed. Damage assessment is usually done by histologic methods, although electrophysiologic approaches, and in the case of non-human primates, psychophysical methods, are also feasible. Pressure elevation is best accomplished by obstructing aqueous humor outflow. For any model, its relevance relies heavily on the normal optic nerve head anatomy of the animal being used.

2.1. Comparative optic nerve head anatomy

The majority of models used today rely on either non-human primates or rodents. Of the rodents, the best described is the rat, although the mouse anatomy is presumed to be similar.

The best-established animal models of IOP-induced optic nerve damage have been developed in non-human primates (Fig. 1). This is primarily due to the close anatomic association these animals have with the human optic nerve head. As in the human, the monkey optic nerve head can be divided into nerve fiber layer, prelaminar, laminar, and retrolaminar regions (Anderson, 1969, 1970). The lamina cribrosa is composed of multiple layers of collagen and elastic tissue that often contain embedded capillaries. In addition, the posterior limit of the lamina cribrosa coincides with the beginning of myelination of the optic nerve fibers.

Earlier studies in non-human primates demonstrated that the connective tissue beams of the lamina cribrosa are composed of several types of interstitial collagen, and typical basement membrane components laminin and collagen type IV (Hernandez et al., 1987; Morrison et al., 1988). These basement membranes are associated with the capillary endothelial cells within the laminar beams, and with the astrocytes lining the beams (Morrison et al., 1989).

At the cellular level, within the lamina cribrosa, processes of astrocytes that line the laminar beams project into the axon bundles. These processes are oriented across the laminar openings. They lie perpendicular to the axons, and provide a rich supportive framework for the axons. Posterior to the lamina, the optic nerve becomes myelinated, and oligodendroglia become the predominant glial cell.

While the rat optic nerve head lacks the monkey's close anatomic similarities to the human, several important similarities do exist. Fig. 2 illustrates a saggital longitudinal section through a normal rat optic nerve head. The neural component of the nerve head, consisting of optic nerve fiber bundles and astrocytes, is shaped like a wine bottle, with a narrow neck, located at the level of the sclera, and an expanding transition zone leading to the retrobulbar optic nerve. The rat optic nerve head appears relatively elongated compared to the primate, and myelination begins approximately 0.5 mm posterior to the sclera, rather than at the posterior edge of the sclera. This appears to coincide with the posterior margin of the transition zone. Scattered patches of connective tissue are seen throughout the transition zone, many of which contain capillaries and may represent a rudimentary lamina cribrosa (Morrison et al., 1995a).

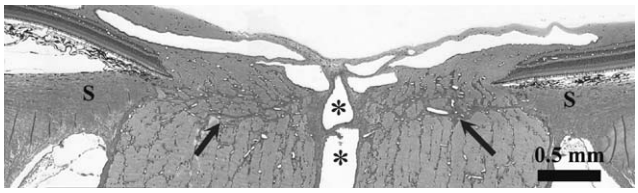

Fig. 1. Longitudinal section of monkey ONH. Arrows indicate lamina cribrosa. Note central retinal vein and artery in middle of the ONH (*), S = Sclera. (Courtesy of Claude Burgoyne, MD.)

In the rat optic nerve head, the sparse collagenous laminar beams of the transition zone have an extracellular composition that is nearly identical to that of the primate, including scattered elastin fibrils (Morrison et al., 1995a). At the ultrastructural level, optic nerve head astrocytes are oriented across the optic nerve head, within the plane of the sclera, and lie perpendicular to the optic nerve axons. Within axon bundles, astrocyte processes are in intimate contact with optic nerve axons, remarkably similar to the situation in the primate ONH (Fig. 3).

The vasculature of the rat optic nerve head also has several similarities to that of the primate, along with some differences (Morrison et al., 1999b; Sugiyama et al., 1999). Casting studies confirm that the primary blood supply to the rat optic nerve head is through the ophthalmic artery (Fig. 4). Immediately beneath the optic nerve, and just posterior to the globe, this artery trifurcates into the central retinal artery, which continues directly into the eye, and two long posterior ciliary arteries that enter the nasal and temporal sclera. As in the primate (Cioffi and Van Buskirk, 1994), the central retinal artery does not supply direct branches to bulk of the optic nerve head, with the exception of a few small capillaries that enter the retinal nerve fiber layer.

Most of the blood supply to the optic nerve head is centripetal, from vessels arising from the posterior ciliary arteries. These branches form a rudimentary circle of Zinn-Haller around the optic nerve head, sending penetrating branches through the choroid into the base of the optic nerve head.

Venous drainage at all levels of the optic nerve head flows into the central retinal vein. However, unlike the primate, this does not occur in a centrifugal pattern. This is primarily because the central retinal vein of the rat eye, like the artery, lies inferior to the nerve head.

Fig. 2. Vertical sagittal section of normal rat ONH. Note narrow "neck" (N) of the optic nerve, adjacent to the sclera (S). The expanding transition zone (T) ends with the myelination of the retrobulbar optic nerve (arrows). Both regions display orderly columns of astrocytes. Central retinal vein (*) is located at inferior margin of the ONH. Arrowheads = capillaries within rudimentary laminar beams.

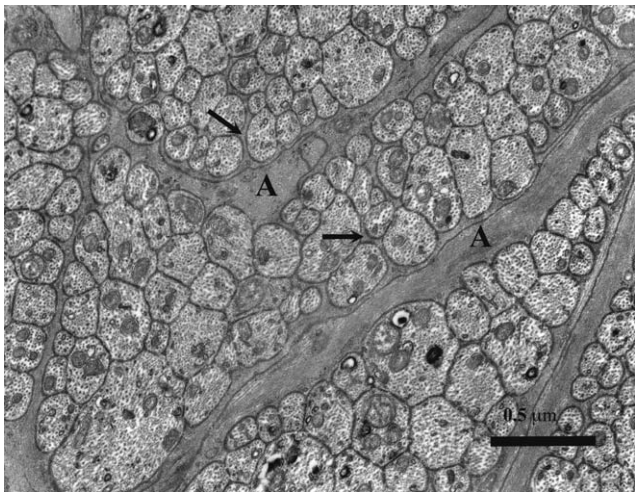

Fig. 3. Transmission electron micrograph of rat ONH 100 μm posterior to Bruch's membrane, at the level of the sclera. Note intimate relationship between astrocyte (A) foot processes (arrows) and axons.

Fig. 4. Schematic representation of arterial supply (dark shading) and venous outflow (lighter shading) in rat ONH. Figure is oriented with retina side down. Note centripetal vascular supply to capillary bed, via branches from posterior ciliary arteries (PCA). Overall, venous outflow at all levels of the nerve head is into the central retinal vein (V), located inferior to the neural tissue. R = Retina vasculature; S = Choroidal venous sinus; A = Central retinal artery; V = Central retinal vein; OA = Ophthalmic artery; NSV = Nerve shealth vein.

This vein originates from the confluence of the major retinal veins. It also receives venous blood from the anterior and transition regions of the nerve head. At the level of the choroid, the central retinal vein joins a broad sinus, which is derived, at least in part, from the choroidal system. Posteriorly, the central retinal vein lies immediately beneath the neural portion of the optic nerve head, along with other large veins in the optic nerve sheath that are connected to the choroidal vasculature.

2.2. Non-human primate models of pressure-induced optic nerve damage

In 1978, Gaasterland described the use of the argon laser to produce scarring of the trabecular meshwork and increase aqueous outflow resistance (Gaasterland and Kupfer, 1974; Gaasterland et al., 1978). Later, Quigley detailed the laser parameters for this method to produce scarring of the aqueous humor outflow while minimizing damage to the ciliary body (Quigley and Hohman, 1983). Since then, many groups have successfully used this method to produce chronically elevated IOP. Other methods have also been described, generally relying on injection of various particulate substances into the anterior chamber, including ghost red blood cells (Quigley and Addicks, 1980) and microspheres (Weber and Zelenak, 2001). All of these cause aqueous humor outflow obstruction, with resultant elevated IOP. However, laser photocoagulation of the trabecular meshwork remains the most popular method in primates.

IOP measurement in non-human primate models is performed by some groups with a modified Goldmann tonometer (Kaufman and Davis, 1980) or, alternatively, with a TonoPen tonometer (Peterson et al., 1996). Others use the pneumatonometer (Toris et al., 2000). Because of handling concerns with these animals, most groups perform such measurements with the aid of a general anesthetic. The most commonly used such agent is ketamine, due to reports that this is the least likely to artifactually lower IOP (Erickson-Lamy et al., 1984). However, selected groups have more recently trained monkeys to allow applanation tonometry in the awake state, using only topical anesthesia (Toris et al., 2003). By avoiding anesthetics, which can have cumulative deleterious effects on the animals and their physiology, accurate measurements are therefore possible, as often as several times a day. These groups report that the IOP response is generally more reproducible with this approach than with general anesthesia. In addition, avoiding general anesthetics makes it easier to detect subtle changes in IOP, as might result from drugs designed to lower IOP.

The intent of these models is to produce a moderate IOP elevation that mimics the IOP seen in human open angle glaucoma. However, most groups have noted a variable elevation in IOP with increased fluctuation following laser treatment. This complicates the interpretation of the resulting optic nerve damage, particularly if the pressure rises high enough to compromise retinal blood flow. To counter this, some groups administer topical pressure-lowering agents to keep the resulting IOP in a predetermined range (Pena et al., 2001).

Assessment of optic nerve and retinal damage in the monkey can be performed histologically using methods similar to those used for human eyes. Many investigators have demonstrated loss of optic nerve axons in this model (Gaasterland and Kupfer, 1974; Gaasterland et al., 1978; Quigley et al., 1987), as well as RGC (Glovinsky et al., 1991). More clinical demonstrations of axon loss with this model result from analysis of the nerve fiber layer in the retina using special fundus photography (Quigley, 1986). These studies have allowed detailed pathologic correlations with retinal and optic nerve tissue, corroborating the value of this clinical observation. Clinical evidence of optic nerve cupping can also be obtained with fundus photography, as well as confocal laser scanning ophthalmoscopy (Burgoyne et al., 2002).

More recently, elegant work with awake, trained rhesus monkeys has documented the development of progressive visual field defects following experimental elevations of IOP (Harwerth et al., 2002, 1999). These studies have been expanded to allow comparison of visual field loss to RGC loss (Harwerth et al., 1999). This model has also been used to study the electrophysiological effects of chronic glaucoma (Frishman et al., 2000).

We have already mentioned the logistic difficulties of obtaining adequate pressure measurements in awake monkeys, and the problems induced by general anesthetics. Other drawbacks of using non-human primate glaucoma models include the expense of purchase and daily maintenance of the animals, and the potential health risk to animal care workers from disease or injury. Finally, because of inter-individual variability, large numbers of animals are required in experiments designed to assess cellular responses of the optic nerve head and retina to IOP. This can be difficult to achieve due to the cost of these animals.

2.3. Rat models of pressure-induced optic nerve damage

For the above reasons, we and other laboratories have long sought to develop and use a less expensive, more manageable model of pressure-induced optic nerve damage. The goals of such a model are to achieve a better understanding of the cellular mechanisms of glaucomatous optic nerve damage and to develop a reliable, cost-effective method of evaluating potential treatments for alleviating optic nerve damage in glaucoma.

In 1993, we first demonstrated the feasibility of measuring IOP in the rat eye using the TonoPen (Moore et al., 1993). Since then, interest in using laboratory rats for understanding the mechanisms of glaucomatous optic nerve damage has grown steadily, and numerous papers have now been published using rat models to understand pressure-induced optic nerve damage.

One anatomic difference between the rat and primate ONH is that the rat lacks a well-developed, collagenous

lamina cribrosa. We feel that this most likely affects regional tissue response to altered IOP. However, the close ultrastructural association between ONH astrocytes and axons are remarkably similar in both species (Fig. 3). Because of this, we feel that rat models are highly relevant for understanding cellular mechanisms of axonal injury from elevated IOP and in glaucoma. Because rats are relatively cost-efficient, many animals can be used per experiment. This minimizes the effects of interanimal variability and improves the validity of the results. In time, conclusions on cellular mechanisms defined with these models can then be tested in the primate model in well-focused experiments. In addition, using adequate numbers of animals is essential for using these models to test the efficacy of potential neuroprotective agents.

2.4. Measurement of IOP in rats

A reliable, unbiased method of measuring IOP is indispensable for working with any model of glaucoma. The goal of measuring IOP is to obtain a sampling of pressures that is adequate to determine the level of IOP that the eye (especially the optic nerve head) is experiencing during the experimental period. This is the only way to find the true relationship between pressure and damage.

2.4.1. Measurement methods

Our approach has been to adapt the use of the hand-held TonoPen tonometer to the rat eye (Moore et al., 1995, 1993). This instrument, developed on the Mackay Marg principle for use in humans, is portable and versatile. Because of this, measurements can be taken with the instrument held in either the horizontal or the vertical position. This allows the observer to measure IOP in animals while they are awake, without using cumbersome restraints or other manipulation. The importance of obtaining awake IOP measurements will be discussed below.

In our initial report, we demonstrated that the TonoPen could be used to measure IOP in the rat eye using animals anesthetized with a general anesthetic (Moore et al., 1993). By measuring pressures in eyes cannulated and simultaneously connected to a pressure transducer, we established that masked measurements with this instrument in these small eyes correlated well with actual IOP (Fig. 5).

Repeated comparisons of simultaneous TonoPen readings with actual pressures derived from a transducer have allowed us to develop a specific set of criteria for deciding if a given IOP reading is valid. In general, valid readings are associated with firm, but not excessive, contact of the instrument tip with the cornea that slightly moves the eye posteriorly. Minimal contact often produces a single digit reading. This is generally

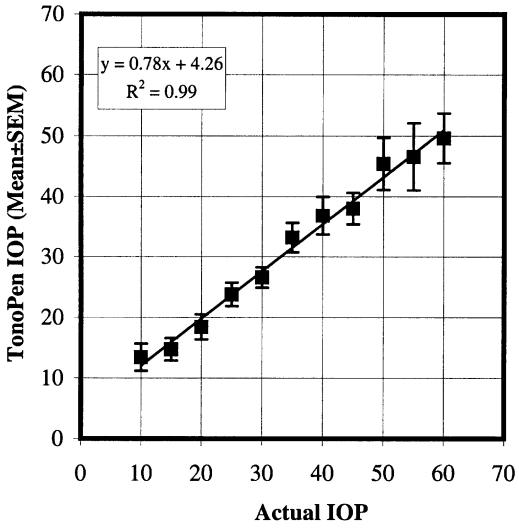

Fig. 5. Calibration curve comparing TonoPen measurements with actual pressures measured with a transducer in the cannulated eye of an anesthetized rat.

due to activation of the instrument by the tear film meniscus, and should be ignored. Similarly, readings occurring as the tip breaks contact with the cornea ("off" readings) are not accurate. Because the instrument is unable to recognize these readings as invalid, the automatic averages that it creates are also unreliable. Instead, we have found that the mean of individual valid readings is a good measure of IOP (Moore et al., 1993). The validity of this method has been demonstrated to us numerous times by the close correlations we find between the pressure readings and nerve damage, and as we study cellular responses to IOP.

We subsequently demonstrated that IOP could be monitored in rats in this manner over time (Moore et al., 1995). However, when measurements were performed as often as every day, animals began to lose weight and their mean IOP decreased. Because of the cumulative side effects of the general anesthetics, and their potential to lower IOP artifactually (Jia et al., 2000a), we began to investigate the possibility of measuring IOP in awake animals, using only topical anesthesia. This approach would provide the most accurate reflection of the level of IOP experienced by the eye.

Danias and coworkers have recently developed another device for rat IOP measurement, the rebound tonometer (Kontiola et al., 2001). Using a pin suspended within a solenoid, IOP is determined based on the rate of deceleration of the pin when it is brought into contact with the cornea. Good correlation has been reported against manometrically determined IOP in cannulated eyes and the TonoPen in anesthetized animals (Goldblum et al., 2002).

Another device adapted for measurement of IOP in rat eyes is the Goldmann tonometer (Cohan and Bohr, 2001a, b; Grozdanic et al., 2003a). This instrument has

been modified for use in both the rat and the mouse eye by increasing the angle of the prisms within the tonometer tip to account for the increased curvature of the cornea. The tonometer strain gauge is also modified to accommodate the reduced corneal rigidity. The tonometer is then mounted on a clinical biomicroscope, with one investigator holding the animal at the tonometer and the other obtaining pressure readings. Calibration studies with this modified instrument using cannulated eyes have indicated a good correlation of tonometer readings with actual, transducer pressures. This method has also been used with animals in a awake state (Cohan and Bohr, 2001a, b). Disadvantages include the necessity of obtaining the modified equipment, as opposed to the TonoPen, which is currently readily available, and the need for two people to work together to obtain the measurements.

The pneumatonometer has also been used for rat IOP measurements (Shareef et al., 1995). This instrument appears to provide recordable pressure readings, and has been used by several investigators. However, its design does not permit reliable calibration in these small eyes, as moderate, sustained contact with the eye is necessary to get a reading. This means that the actual pressure within the eye will be significantly affected during the calibration.

Although there are several instruments for measuring IOP in rat eyes, the majority of publications studying chronically elevated pressure in rats are performed using the TonoPen. This instrument is readily available and does not need to be modified for use in rats. It is easily and reproducibly calibrated. Once the skill of use in these small eyes is mastered, the TonoPen provides reliable determinations of IOP (Moore et al., 1996).

2.4.2. *Characteristics of IOP in rats*

In many animals, IOP can fluctuate by several mm Hg over the course of a 24 hour day. In rabbits, pressure peaks occur during the dark phase of the cycle, and this can be entrained by changes in the light cycle apparently tied to fluctuation in aqueous humor formation (Gregory et al., 1985; McLaren et al., 1996). We reasoned that, if we could demonstrate a circadian fluctuation to IOP in awake rats with the TonoPen, this would indicate that these pressure measurements were meaningful and sensitive.

We found in Brown Norway rats a distinct circadian fluctuation in IOP that was repeatable and dependent on the light cycle (Moore et al., 1996). Initially, animals demonstrated low pressures during the light portion of the cycle, and peak pressures occurred during the dark. When the light and dark phases of the light cycle were reversed, the IOP cycle also reversed, following several days of re-equilibration. This suggested that the IOP curve is a true circadian phenomenon, entrained by the light cycle. In addition, when placed in constant dark, the animals continued to demonstrate a similar circadian fluctuation. We concluded that physiologically meaningful, sensitive IOP measurements could be reliably obtained in awake rats.

The effect of this circadian variation has important implications for the use of outflow obstruction glaucoma models. We monitored awake IOP during both the light and the dark phase of the circadian cycle in animals with aqueous outflow obstruction and compared these measurements to the extent of damage found in optic nerve cross sections (Jia et al., 2000b). Thirty-six percent of glaucoma eyes with optic nerve injury had no significant light phase IOP elevation, while 100% of these eyes had significant elevation during the dark phase. In some glaucoma eyes, the dark phase IOP was 20 mm Hg above that measured during the light phase. This accentuated fluctuation probably represents an exaggeration of dark phase elevation, since it is superimposed on experimental outflow pathway sclerosis. This is likely similar to the increased IOP fluctuation reported in human glaucoma (Asrani et al., 2000; Konstas et al., 1997). It is clear that, when animals with experimental outflow obstruction are housed in standard lighting conditions, IOP must be monitored in the dark phase as well as the light.

However, such frequent measurement of IOP can be cumbersome. In addition, the large IOP fluctuation that these eyes can experience may complicate efforts to correlate pressure history to optic nerve damage. For this reason, we sought to minimize the underlying IOP fluctuation using a low level constant light environment, which has previously been reported to reduce circadian IOP changes in other species (Rowland et al., 1981).

To accomplish this, we housed Brown Norway rats initially in standard lighting conditions, with lights automatically turned on at 6 AM (light phase) and off at 6 PM (dark phase). Animals received hypertonic episcleral vein injections, and then were placed in constant light conditions consisting of 24-h exposure to low-level (40–90 lux) fluorescent lighting for 35 days. Daily IOP readings were made alternately between 9–11 AM (AM IOP mean) and 7–9 PM (PM IOP mean) throughout the experiment.

Light and dark phase IOP for untreated eyes ($N = 7$) in standard lighting was 21.3 ± 1.1 (mean $\pm$ S.D.) and 30.7 ± 0.7 mm Hg, respectively. After one week in constant light, AM and PM IOP readings became indistinguishable. Fellow eyes at 7 days had AM and PM IOP readings of 27 ± 1 and 26 ± 2 mm Hg, respectively, while the corresponding mean IOPs for the periods from 7 to 35 days was 27 ± 2 and 28 ± 2 mm Hg, respectively.

IOP in the glaucoma eyes became significantly elevated over that in the fellow eyes. Mean AM and PM IOP of all glaucoma eyes was 39 ± 6 and 40 ± 6 mm Hg, respectively. In addition, mean values obtained

from AM or PM readings for individual glaucoma eyes differed by only $3 \pm 4\%$, regardless of the time of day at which they were taken. We have found the use of this constant light paradigm extremely useful in this model. Comparison of mean IOP to optic nerve damage using a grading system (described below) has consistently shown an excellent correlation between these parameters (Fig. 6).

We have housed normal Brown Norway rats in constant light for as long as 12 months. The pressure effects are maintained throughout the entire period. Histologically, the retinas were normal and indistinguishable from retinas of five, age-matched animals housed under standard light:dark conditions for the same time period (Fig. 7). (LaVail et al., 1997). Outer nuclear layer thickness measurements, determined by Dr. Matt LaVail, for constant ($N = 4$) and standard lighting ($N = 3$), were 29.3 ± 2.7 and $28.9 \pm 3.4\,\mu m$, respectively. This resistance to light-induced photoreceptor loss is most likely due to the low level of light used, and the fact that these animals are pigmented (LaVail, 1980).

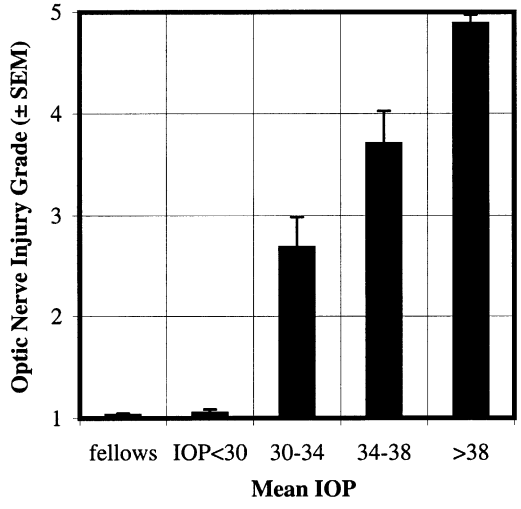

Fig. 6. Relationship between mean IOP and ON damage (determined by injury grade) in rats housed in low level constant light following hypertonic saline injection.

2.5. Assessing optic nerve damage

Assessing damage to the optic nerve is as critical as IOP measurement to understanding the relationship between pressure and damage. Optic nerve damage in human glaucomatous eyes and monkeys with experimental glaucoma has been traditionally determined by light microscopic evaluation of optic nerve cross sections. The advantages of this approach are that all of the output from the retinal ganglion cells can be assessed in a single tissue section. Well-established, semi-automated methods using image analysis systems exist for determining total numbers of axons, using fellow, or normal optic nerves as controls (Quigley et al., 1987). In this fashion, loss of axons is determined as the number of remaining axons compared to that seen in a normal nerve. An additional advantage of this approach is that relatively few manipulations are required. This reduces the potential for errors and unintended bias.

A disadvantage of counting axons in optic nerve cross sections by light microscopy is that the quality of the axon estimates is closely tied to the quality of tissue fixation. This is a major problem in evaluating human glaucoma specimens, where time to fixation is often variable. It is less of a concern in animal models in which perfusion fixation can be performed, or the tissues immediately placed in fixative following enucleation.

Transmission electron microscopy (TEM) can also be used to count axons in optic nerve cross sections (Chauhan et al., 2002). Here, tissue sections from experimental and control nerves are photographed in random, standardized fashion and axon counts are performed manually. At this level, the axons can be identified by their myelin sheaths and contained microtubules. Degenerating axons are identified by swollen

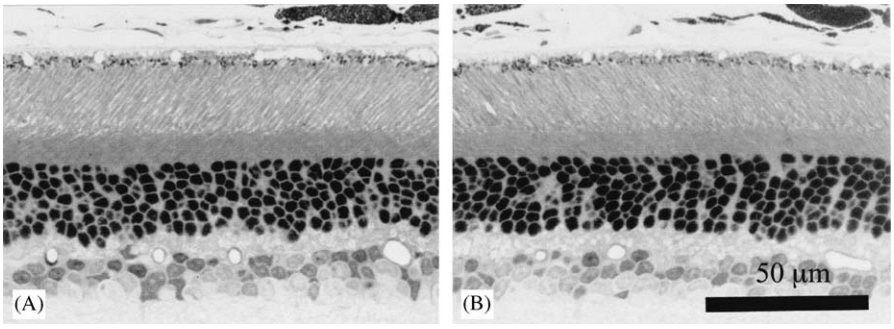

Fig. 7. Light micrographs of plastic-embedded sections of Brown Norway rat retinas maintained in either constant light (A) or standard light (B) for one year. Both retinas are from the equatorial of the eye and are normal and indistinguishable. Toluidine blue stain. 560X Courtesy of Matt Lavail Ph.D.

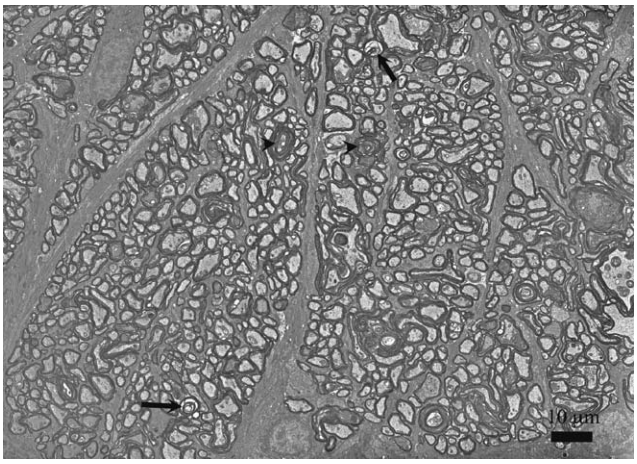

Fig. 8. Transmission electron micrograph of myelinated rat optic nerve from eye with chronic IOP elevation following hypertonic saline injection. Axonal degeneration is identified by swollen axonal profiles, disorganized neurofilaments (arrows), or collapsed myelin sheaths (arrowheads). Many axons, however, appear normal.

profiles, absence of neurofilaments, or myelin debris (Fig. 8).

We have performed a direct comparison of this transmission electron microscopic method to counts performed by a semiautomated, light microscopic method. For TEM analysis, optic nerve cross sections from 4 normal rats were placed on 300 mesh grids and photographed at 1000× and printed at 3000×. Each photograph occupied approximately 65% of a grid square opening. Axon counts of all photographs were performed manually and the resulting density extrapolated to total axon counts using the total optic nerve area measured in a 530× photograph. For light microscopy, a method previously used for quantitative examination of glaucomatous human and primate optic nerves was modified for use on rat optic nerves (Quigley et al., 1987). An IBAS image analysis system (Carl Zeiss, Germany) was used to count axons (identified by their myelin profiles) in each of 24 rectangular areas distributed over the nerve cross section.

The mean axon count (in thousands) obtained by the TEM method for these eyes was 126.4 ± 7.8 ($\pm$SD), as compared to 86.8 ± 11.5 by LM, a statistically significant difference ($p < 0.02$, Student's t-test). The mean difference between these methods was 39.6 ± 19.4 thousand axons, or $31 \pm 15\%$ of the TEM count. The extent of underestimation by the LM method ranged from 19% to as high as 43%. While the reasons for this rather large discrepancy are unclear, we suspect that many optic nerve axons in the rat are smaller than the practical limits of their resolution by light microscopy and do not get counted by the software of the image analysis system. It should be noted that the range of this underestimate is fairly large and the relationship between the two methods is not linear. Thus, it may be difficult to simply extrapolate measurements from one method to the other.

2.5.1. Qualitative assessment of optic nerve damage

In spite of the greater accuracy of the TEM method, it is clearly too labor intensive for use with large numbers of eyes, often required for tissue and drug studies. For these purposes, we have developed a sensitive light microscopic method for using optic nerve cross sections to determine optic nerve damage (Jia et al., 2000b). This involves assessment of axon degeneration and grading injury as a function of the extent of optic nerve involvement. With light microscopy, axonal degeneration can be identified by the appearance of swollen axons that lack apparent axoplasm, and dark axons due to collapsed myelin sheaths (Fig. 9). In this system, a grade 1 nerve is normal; grade 2 a focal region of degeneration; grade 3 is degeneration spreading beyond the focal region; grade 4 is degeneration involving the entire cross section of the nerve, with approximately equal numbers of apparently normal and degenerating axons; and grade 5 is apparent degeneration of all axons. Using multiple examiners unaware of IOP history, each recording an injury grade, it is possible to calculate a mean injury grade for each nerve. Other investigators, working with albino animals and animals with chronic ischemia, have developed and used similar qualitative damage scales (Levkovitch-Verbin et al., 2002a, b; Archibald and Chauhan, 2003).

Fig. 10 is a graph of optic nerve damage in a group of experimental optic nerves and their normal fellows as determined with this grading system, compared to a

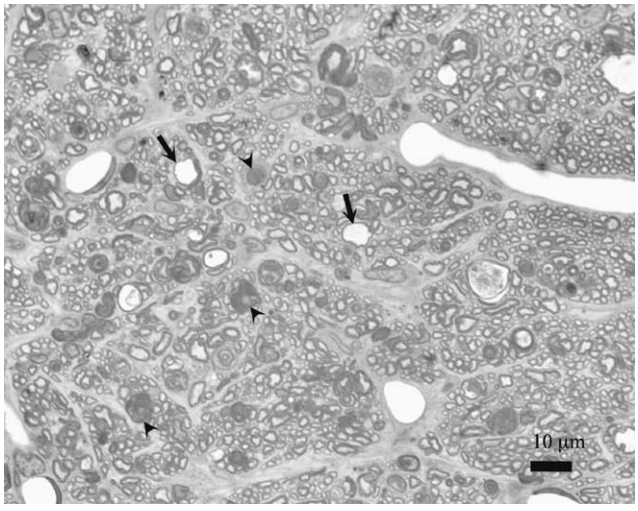

Fig. 9. Light micrograph of axonal degeneration in myelinated optic nerve. Degenerating axons appear swollen and empty (arrows) or dark due to collapsed myelin sheaths (arrowheads).

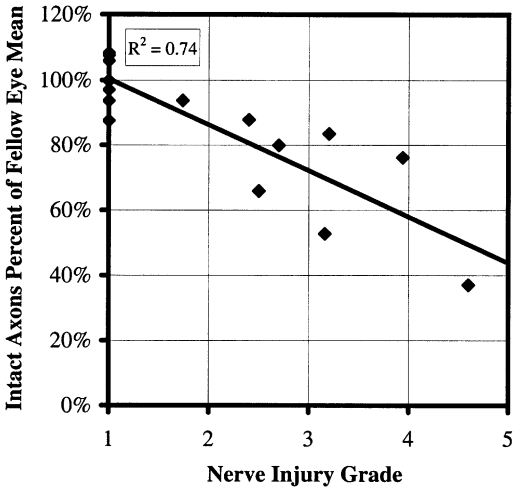

Fig. 10. Graph comparing damage from experimental and fellow eye optic nerves from 8 animals as determined by ultrastructural assessment of axon counts and a qualitative, light microscopic grading system. Axon counts (expressed as a percentage of the mean counts of normal fellow eyes) appear on the *y*-axis and mean optic nerve injury grade of 5 masked observers is on the *x*-axis. Linear correlation between the two methods was good ($R^2 = 0.74$).

systematic ultrastructural determination of axon counts (described above) in the same nerves. In this graph, axon counts are expressed as a percentage of the mean counts of normal fellow eyes as a group. A linear relationship exists between the two methods, supporting the reliability of the grading system.

This analysis also indicates that the grading system is more sensitive than one using total axon counts compared to fellow, normal optic nerves. The axon counts of the fellow eyes are arrayed along the *y*-axis, corresponding to a grade of 1, or no damage. This shows that the natural variation in axon counts between these normal eyes can range as much as 20%. Yet some eyes with a mild nerve injury (grade 2–2.5) clearly have axon counts that are within this normal range, suggesting that this method is relatively insensitive to mild damage, compared to the grading system. Finally, this graph also shows that nerves with advanced damage (grade 4 and above) may not have complete loss of axons. Several of these nerves correspond to axon counts that are 30–40% less than their fellow nerves, but still retain substantial numbers of axons when studied by TEM.

2.6. Determining RGC loss

Counting retinal ganglion cells is another common method for assessing damage. In this approach, a tracer, such as fluorogold, is applied to or injected into the superior colliculus or placed in contact with the cut stump of the optic nerve attached to the globe. The tracer is then transported by retrograde axoplasmic flow to the RGC cell body over several days. Retinal flat mounts are then prepared, and labeled RGC are counted in systematic fashion in representative regions of the retina. RGC loss can be expressed as a reduction in labeled cell density in the fields examined or by measuring total retinal area and then extrapolating counts to obtain total viable RGC in the retina and comparing this to counts in fellow eyes.

The advantage of this technique is that, because it relies on axonal transport, it assesses viable cells; RGC still present within the retina but without functional axons will not be counted. Disadvantages of this technique are that it relies on uniform uptake of the tracer by axon terminals. Another potential disadvantage is that the distribution of RGC may not be uniform in damaged eyes. In this situation, counting RGC in only specified regions may miss regions of high RGC loss. Danias and coworkers have approached this problem by counting labeled RGC in the entire retina using an automated microscope stage (Danias et al., 2002). Even with this advance, however, the increased thickness of RGC within the central part of the retina produces some uncertainty, as it may be difficult to distinguish one RGC from another in flat mounts when they are present in two or more layers.

2.7. Methods of elevating IOP in rats

Over the past 10 years, three general methods of creating chronically elevated IOP in rats have been described. These involve injecting hypertonic saline into the aqueous humor outflow pathways, obstructing outflow by using a laser to scar these limbal outflow pathways, and using cautery to close off venous outflow from the eye.

The primary goal of any experimental method to create chronic pressure elevation is to inhibit aqueous humor outflow without interfering with the eye's ability to produce aqueous humor. The close anatomic proximity of the aqueous humor outflow pathways and the ciliary body pose a particular challenge in the rat eye.

2.7.1. Hypertonic saline injection of aqueous humor outflow pathways

Sclerosis of aqueous humor outflow using hypertonic saline relies on the anatomy of the aqueous humor outflow pathways (Morrison et al., 1995b). As in the primate, the anterior chamber angle of the rat eye has a prominent circumferential channel, analogous to Schlemm's canal, that is bordered internally by the trabecular meshwork. Numerous collector channels lead from this canal through the sclera to a plexus of aqueous veins that lie within the episclera at the limbus. Radially oriented veins travel posteriorly from this plexus within the episclera, to empty into the veins of the orbit.

The hypertonic saline method produces scarring of the anterior chamber angle while minimizing ciliary

body damage by injecting the saline toward the limbus into one of the radial veins within the episclera (Morrison et al., 1997b). A plastic ring is placed around the equator of the eye to confine the injection to the limbus and thus drive the saline into Schlemm's canal and across the trabecular meshwork. The resulting inflammation produces scarring of the meshwork and the anterior chamber angle. The extent of this scarring determines the degree of the pressure rise.

The efficiency with which this technique produces a pressure rise depends greatly on the extent and density of the resulting scarring of the anterior chamber angle. This is influenced by the anatomy of the limbal plexus and how effectively the ring confines the hypertonic saline to the limbus. In general, sustained elevation of IOP occurs 7–10 days following the injection. This is presumably when the scarring process matures and inflammation subsides, allowing resumption of normal production of aqueous humor. In our original description, a second injection was performed in 7 out of 20 consecutive eyes injected with 1.75 M saline. (Morrison et al., 1997b) While some investigators routinely perform a second injection in all animals (Chauhan et al., 2002) we and others (Hanninen et al., 2002) have found it sufficient to perform the second injection only if an IOP rise does not occur within the first 2 weeks. Modifications of the ring, designed to better control the access of saline to specific portions of the trabecular meshwork are currently underway to minimize pronounced elevations of IOP and reduce the need for subsequent injections.

The duration of elevation with this technique is generally dictated by the protocol of the experiment being performed. In our experience, we found that injections of saline with concentration higher than 2.0 M produced marked elevation of IOP that could remain highly elevated in many eyes for prolonged periods, up to several months (Johnson et al., 2000a, b; Morrison et al., 1997b). In an effort to reduce the extent of pressure elevation, saline concentrations lower than 2.0 M were found to produce a more moderate pressure elevation. Generally, the majority of our experiments have been limited to 6 weeks, and the animals deliberately sacrificed for specific histologic or cell biology study. Other investigators have reported durations of elevated IOP with this method as long as 12 weeks (Chauhan et al., 2002; Hanninen et al., 2002; McKinnon et al., 2002a). If allowed to survive, the IOP can remain elevated in many animals beyond this time point.

The saline injection method generally produces a range of IOP response, from a minimal, but statistically significant rise above the fellow eye to a level reaching two-fold or more above normal. We have found this range useful, as it allows us to evaluate the retina or optic nerve head response over several levels of IOP. Frequently, changes seen will be closely associated with the mean level of IOP. Damage can also be correlated with peak IOP elevation (Chauhan et al., 2002) and with overall IOP exposure, expressed in terms of days of pressure elevation above normal (Chauhan et al., 2002; McKinnon et al., 2002a).

2.7.2. Limbal laser treatment

Another method to produce elevated IOP in rats uses external laser to the limbus. This technique was initially described using injection of India ink into the anterior chamber, allowing time for it to enter the angle structures, followed by photocoagulation of the limbus with the argon laser (Ueda et al., 1998). The India ink apparently improves the uptake of the laser energy. Histologically, phagocytosis of the ink particles was identified in the chamber angle, in addition to closure of the chamber angle. Other groups have also achieved significant elevations of IOP using similar laser treatment, but without injection of foreign materials into the anterior chamber (Levkovitch-Verbin et al., 2002b; WoldeMussie et al., 2001).

Histologic descriptions suggest that the effects of this laser treatment are to coagulate the limbal vasculature and produce chronic angle closure (Levkovitch-Verbin et al., 2002b; Ueda et al., 1998). Both of these effects could increase the resistance to aqueous humor outflow. However, Levkovitch-Verbin and colleagues, using the diode laser, specifically evaluated the effect of treating limbal vessels alone vs. treatment of the trabecular meshwork and anterior chamber angle (Levkovitch-Verbin et al., 2002b). They found that specific treatment of the angle was necessary to achieve chronic elevation of IOP. This further supports the conclusion that significant pressure elevations depend upon sclerosis of the trabecular meshwork and angle closure. We suspect that collateral injury and scarring of the anterior chamber angle is largely responsible for the subsequent IOP rise following laser treatment of the limbal vasculature alone (WoldeMussie et al., 2001).

Nearly all published descriptions of this technique use non-pigmented animals. This is mostly due to the fact that such treatment in pigmented eyes produces a dramatic inflammatory response, with possible ocular effects that are beyond just that needed to cause angle closure. This would have a significant impact on the accuracy of IOP measurement with this method, since, in our experience, it is quite difficult to obtain awake IOP measurements on non-pigmented animals.

Most variations of this technique produce an abrupt increase in IOP, present at the first pressure measurement after the laser treatment. Following this, the pressure appears to diminish gradually over several weeks. A specific evaluation of the effects of a single laser treatment showed that IOP returned to baseline by 3 weeks (Levkovitch-Verbin et al., 2002b). Subsequent

work by this group, in which they were able to follow eyes with IOP elevation for as long as 9 weeks, used an additional laser treatment as needed (Martin et al., 2003). Other groups routinely perform a second treatment between 1 and 3 weeks after the first (Bakalash et al., 2002; Ishii et al., 2003; Schori et al., 2001). With this, the duration of pressure elevation has been reported to continue for as long as 8 weeks, culminating in planned sacrifice.

2.7.3. Episcleral vein cautery

The third method of creating elevated IOP in rats consists of cauterizing one or more of 4 large episcleral veins, located just posterior to the rectus muscle insertions (Sawada and Neufeld, 1999; Shareef et al., 1995). As in the initial description of this technique, the majority of studies using this model will cauterize 3 of these vessels. Because these vessels connect to episcleral veins that drain aqueous humor from the limbal plexus, this treatment is thought by some investigators to produce elevated IOP by reducing aqueous humor outflow, similar to elevated episcleral venous pressure glaucoma in humans (Shareef et al., 1995). However, IOP increase following this procedure has been noted to rise immediately after cauterization, suggesting that other mechanisms may contribute to the pressure response. Other investigators have determined that these vessels are most likely vortex veins (Grozdanic et al., 2003b). In rats, vortex veins receive blood from more than just the episcleral veins. This includes a majority of the choroid as well as the anterior uvea (Morrison et al., 1987, 1999b). Thus, it is likely that, following cauterization of these veins, arterial blood is suddenly left with insufficient outflow from the globe. This would rapidly produce significant ocular venous congestion, which is consistent with an immediate rise in IOP (Goldblum and Mittag, 2002).

This procedure appears to work in pigmented and non-pigmented animals (Grozdanic et al., 2003b). However, the effectiveness of this technique in producing chronic pressure elevation appears to be variable. Several groups have documented pressure elevations for periods as long as 5 and 6 weeks (Shareef et al., 1995), with IOP returning to normal in 30% of animals after 2–4 weeks (Ahmed et al., 2001). Grozdanic reported that IOP gradually returned to normal over 8 weeks (Grozdanic et al., 2003b). Others have found that IOP will remain reliably elevated for as many as 6 and 7 months without retreatment (Neufeld et al., 1999, 2002).

Mittag noted that IOP returned to normal 3 weeks after 3-vessel cauterization in all animals (Mittag et al., 2000). Only by giving concomitant 5 fluorouracil injections were they able to achieve a sustained IOP elevation. Presumably, the antimetabolite inhibits formation of collateral vessels, which otherwise shunt blood out of the eye to reduce the congestion, and the measured IOP.

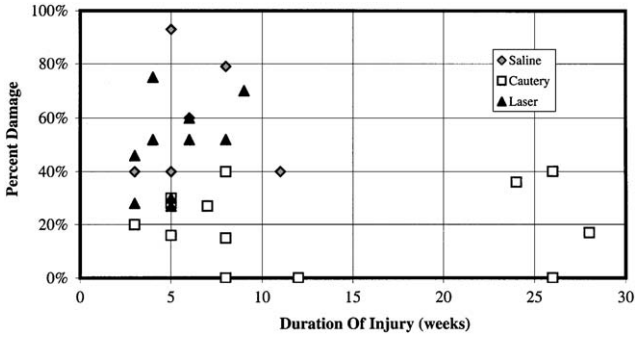

Fig. 11. Comparison of percent damage, from either optic nerve axon count or RGC survival analysis, among different animal model studies as a function of duration of pressure elevation. Extent of pressure elevations ranges from 1.3 to 2.0 times normal.

2.8. Comparison of rat glaucoma models

While the marked increase in interest in using rats to model glaucomatous optic nerve damage is encouraging, these models may not all be equivalent. Direct comparisons are difficult, as methods of assessing IOP and the extent of optic nerve damage are not consistently used for all studies. However, within the parameters of the methods used for each, it is possible to determine a percent optic nerve damage (or loss of RGC) vs. duration of elevation. By graphing this relationship for all available studies using these different techniques, it is possible compare the relationship between duration of elevated IOP and damage for each.

Fig. 11 displays this comparison for various studies from all 3 models for different degrees of pressure elevation (references in Table 1). Because these studies span different time frames, duration is graphed on the horizontal axis, and extent of damage displayed on the vertical axis. Within each model group, there are studies that, taken together, represent more than just one method of assessing IOP and RGC damage. For each model, the extent of pressure elevation in these studies ranged from 1.3× to 2× normal. A sub-analysis of these studies grouped by extent of IOP elevation did not show any differences compared to the results shown here.

From this graph, the hypertonic saline injection and laser models appear to produce an equivalent range of optic nerve and retina damage, from approximately 30% to over 80% over time periods of 3–11 weeks. By contrast, maximum damage reported with the cautery model damage over a similar time frame is 40%, with the bulk of studies showing damage below 30%. In two studies using the cautery model, no damage was found

Table 1
Comparison of rat glaucoma models

Method	Elevation × normal	Duration (weeks)	% Damage	Reference
Hypertonic saline	2	5	93	Hanninen et al. (2002)
	1.4	11	40	Hanninen et al. (2002)
	1.7	8	79	McKinnon et al. (2002a, b)
	1.3	5	40	Schlamp et al. (2001)
	1.3	5	40	Morrison et al. (1997)
	1.3	3	40	Morrison et al. (1998)
	1.5	6	60	Chauhan et al. (2002)
Cautery	2	3	20	Ahmed et al. (2001)
	2	5	30	Ahmed et al. (2001)
	2	5	16	Ko et al. (2001)
	2	7	27	Ko et al. (2001)
	1.7	24	36	Neufeld et al. (1999)
	1.6	8	0 (central)	Sawada and Neufeld (1999)
	1.6	8	15 (periph)	Sawada and Neufeld (1999)
	1.6	26	0 (central)	Sawada and Neufeld (1999)
	1.6	26	40 (periph)	Sawada and Neufeld (1999)
	2	5	28	Ko et al. (2001)
	2	12	0	Mittag et al. (2000)
	1.6	8	40	Naskar et al. (2002)
	1.5	8	0	Grozdanic et al. (2003a, b)
	1.8	28	17	Neufeld et al. (2002)
Laser	2	3	28	Schori et al. (2001)
	2	5	30	Siu et al. (2002)
	1.5	6	52	Bakalash et al. (2002)
	1.7	3	46	Bakalash et al. (2002)
	1.6	5	27	Ishii et al. (2003)
	1.3	4	75	Martin et al. (2002)
	1.23	6	60	Levkovitch-Verbin et al. (2002a, b)
	1.23	9	70	Levkovitch-Verbin et al. (2002a, b)
	1.3	4	52	Martin et al. (2003)
	1.5	8	52	Park et al. (2001)

(Grozdanic et al., 2003b; Mittag et al., 2000). Other studies using this technique have assessed RGC loss after periods of IOP elevation for as long as 26 weeks, finding at most 40% damage in the peripheral retina, and none in the central regions (Neufeld et al., 1999; Sawada and Neufeld, 1999).

From these comparisons, it appears that elevated pressure in the cautery model produces less injury than would be expected by the same approximate elevation produced by either of the other two methods. It is possible that damage in this model is due to ischemia (Goldblum and Mittag, 2002; Grozdanic et al., 2003b). This is supported by Bayer's observation that a-wave amplitude was diminished with little RGC loss in this model (Bayer et al., 2001). These authors suggest that this significant involvement of the outer retina may be due to choroidal insufficiency.

This difference in apparent IOP susceptibility also suggests that the mechanism of the pressure elevation is different in this model. Since the choroid and veins surrounding the ONH are intimately related (Morrison et al., 1997a), congestion of these vessels may provide mechanical protection for the nerve fibers from altered stresses induced by stretch in the adjacent sclera, as opposed to models where elevated IOP is due primarily to aqueous humor outflow obstruction.

Another comparison among these models available in the literature is the pattern of injury. In the initial description of the hypertonic saline model, we noted that in 70% of eyes with a partial optic nerve injury, the damage was located in the superior temporal region of the optic nerve (Morrison et al., 1997b). In a subsequent analysis in a large number of such nerves, we confirmed that the majority of these lesions were indeed within the superior nerve (Morrison et al., 2002). Careful ultrastructural analysis of nerve heads of these animals demonstrated that loss of axons and associated astrocyte changes were located within the superior region of the nerve head, at the level of the sclera. This finding is in agreement with studies of the laser model, analyzed by uptake of fluorogold tracer in the RGC (Wolde-Mussie et al., 2001). Using retinal flat mounts, they

found the most significant reduction of retinal ganglion cells in the superior retina.

In both the hypertonic saline and laser models, IOP elevation is due to aqueous humor outflow obstruction. We surmise that preferential damage to the superior region of the optic nerve head, and superior retinal ganglion cell loss, is a characteristic of elevated IOP produced in this manner. It is possible that transmission of this pressure to the entire sclera produces optic nerve damage. Preferential injury to the superior region of the ONH would then be dictated by the anatomic relationships between the optic nerve head and the adjacent sclera.

Reports to date on the vein cautery model indicate that preferential RGC loss occurs in the peripheral regions of the retina, with less, or even little apparent injury to the central retina (Ko et al., 2001; Sawada and Neufeld, 1999). There is no report of a superior predilection for injury in these studies, although such a pattern has not specifically been investigated and cannot be ruled out.

3. Effects of elevated IOP on the optic nerve head

Studies of human glaucoma specimens suggest that the clinical appearance of cupping results from posterior bowing of the lamina cribrosa and loss of nerve fibers (Quigley et al., 1981; Quigley and Green, 1979). Pathologic studies of glaucomatous optic nerves have demonstrated that there is significant disorganization of the cellular structures within the nerve head, with loss of the normal orderly arrangement of axon bundles, connective tissue laminar beams and supporting astrocytes (Hernandez, 2000; Hernandez et al., 1990; Quigley et al., 1991, 1983). Animal model work confirms this observation and information to date suggests that chronic IOP elevation can produce both axonal and non-axonal changes. Many of these alterations could be unique to this form of damage.

3.1. Axonal changes in the optic nerve head

The most obvious axonal change that occurs following elevation of IOP is loss of the axons themselves. As presented above, this is most readily apparent by assessment of optic nerve cross sections, where increased numbers of degenerated axons can be seen, and through reduced axonal counts in optic nerve cross sections. In our model, degenerating axons are also apparent within the ONH itself (Fig. 12), and have been detected in increased numbers within the superior region in eyes with early optic nerve damage (Morrison et al., 2002).

Disrupted axonal transport appears to be an important axonal effect in eyes with elevated IOP.

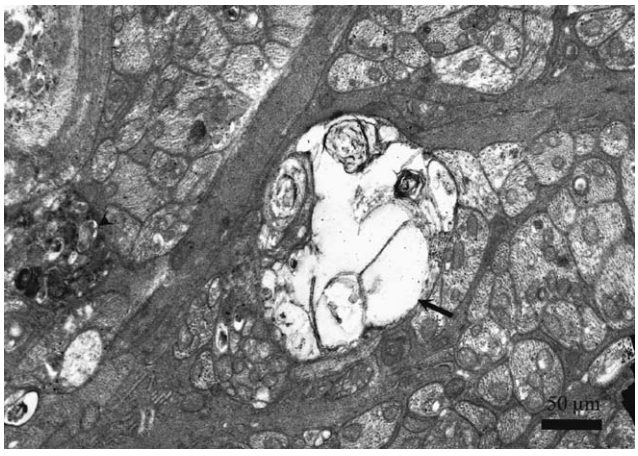

Fig. 12. Transmission electron micrograph of axonal degeneration in the optic nerve head of a rat with moderate IOP elevation. Several axons (arrow) appear to have lost their normal axoplasm, with increased vesicles present in adjacent axons (arrowhead). Note presence of many normal appearing axons.

Ultrastructural analysis of human glaucomatous ONH demonstrated significant axonal swelling, filled with vesicles and mitochondria, in close association with lamina cribrosa beams (Quigley et al., 1981). Although such findings were long presumed to reflect axonal transport obstruction, this was first clearly demonstrated in monkey eyes with acutely elevated IOP (Anderson and Hendrickson, 1974; Quigley and Anderson, 1976, 1977). By labeling RGC with tritiated thymidine, increased accumulations of labeled material were identified within the lamina cribrosa by light microscopy. Minckler used a similar system to demonstrate obstruction of both retrograde and orthograde axonal transport (Minckler et al., 1977). In rat eyes with chronically elevated IOP, we have also noted swollen axons within the ONH, filled with vesicular material consistent with both axon transport obstruction and axonal degeneration (Morrison et al., 1997b).

Investigators have suggested that axonal transport obstruction may lead to RGC death by interrupting the delivery of neurotrophins from the superior colliculus to the cell body of the RGC (Quigley, 1995, 1999). Loss of this communication, vital to the survival of the cell, would lead to cell death. We have identified in rat eyes with elevated IOP a near complete absence of label by immunohistochemistry for neurotrophins BDNF and NT/4-5 within the ONH (Johnson et al., 2000a, b). In animals with acutely elevated IOP, retrograde transport of labeled trkB, the neurotrophin receptor for BDNF, is also interrupted at the level of the ONH (Pease et al., 2000). Thus, altered axonal transport appears to interfere with both retrograde and anterograde transport of neurotrophins vital to the maintenance of RGC. Retinal aspects of this theory will be discussed further below.

3.2. Non-axonal changes in the optic nerve head

3.2.1. Optic nerve head extracellular matrix changes

A prominent non-axonal change in eyes with chronically elevated IOP is the abnormal deposition of extracellular matrix materials within the optic nerve head. Pathologic studies of human glaucoma tissue have demonstrated that these consist of several types of collagen and basement membrane materials, as well as elastin (Hernandez, 2000; Hernandez et al., 1990). Using light and electron microscopy of monkey ONH with experimental elevations of IOP, it has also been demonstrated that these deposits consist of several interstitial collagens and basement membrane components (Morrison et al., 1990b). These changes were found within the laminar pores, in spaces normally occupied by axon bundles. In contrast, transection of the retrobulbar optic nerve head failed to produce similar accumulations. This strongly implies that many of the extracellular changes characteristic of glaucomatous optic nerve damage are a consequence of chronically elevated IOP, rather than simply a response to axonal loss.

Similar studies in the hypertonic saline rat model confirm that these changes are not unique to the primate. Immunohistochemical analysis has demonstrated abnormal accumulations of collagen types I and III, as well as type VI and laminin within the optic nerve head, apparently replacing normal axon bundles (Johnson et al., 1996). As in the primate, these are accompanied by a significant loss of the normal arrangement of astrocytes and optic nerve fiber bundles (Fig. 13). Chauhan, using the same model, has documented sequential and progressive cupping by in vivo confocal microscopy, although only after significant elevations of IOP and in association with loss of over 55% of the axons (Chauhan et al., 2002).

The exact role that these connective tissue and extracellular matrix changes play in glaucomatous optic nerve damage is unknown. It is possible that such changes are an integral part of the cascade of events that leads to axonal damage and retinal ganglion cell loss. Alternatively, they may merely be a parallel consequence of other events, along with axonal injury. However, it is likely that the abnormal extracellular matrix materials can alter the physical behavior of the optic nerve head, particularly in response to changes in IOP.

Burgoyne has shown in non-human primates with elevated IOP that, using confocal scanning laser ophthalmoscopy, it is possible to document changes in the physical response of the ONH surface to acute elevations in IOP (Burgoyne et al., 1995a, b; Heickell et al., 2001). Raising IOP over a several minute period produces a backward movement of the ONH, which then returns to the baseline position after the IOP is reduced to normal. This is termed compliance. Using serial ''compliance testing'' following initiation of chronically elevated IOP with trabecular meshwork laser in monkeys, he has demonstrated that the ONH will initially develop hypercompliance, with greater than usual posterior movement. Later, compliance returns to the baseline state (Burgoyne et al., 1995a).

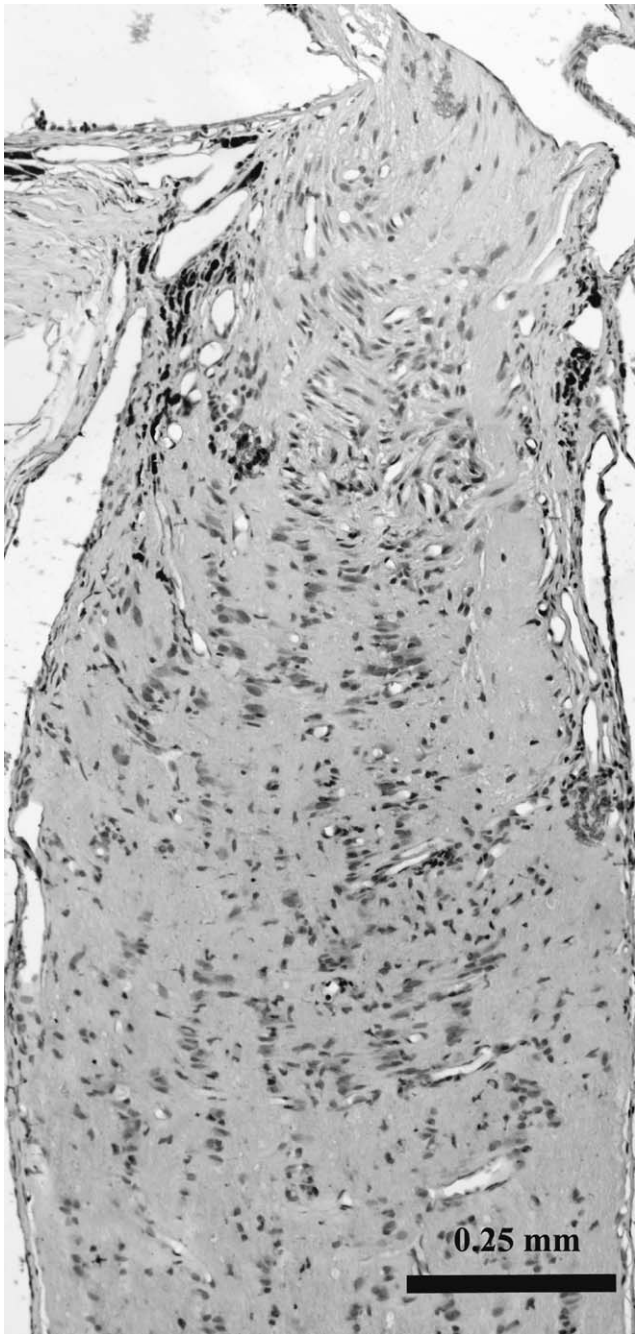

Fig. 13. Light micrograph of rat optic nerve head with moderate IOP elevation and optic nerve damage. Note disorganization of astrocyte nuclei and axonal bundles, along with increased cellularity as compared to normal appearance in Fig. 2.

We believe it is likely that the initial hypercompliance, which Burgoyne and colleagues consider a biomechanical marker of early glaucomatous nerve damage, may result from the initial disorganization of structure of the ONH. This likely results from astrocyte migration and reduced cellular organization (Hernandez, 2000; Tezel et al., 2001). The reduced compliance that accompanies prolonged pressure elevation may reflect the deposition of ECM materials within the ONH. Given this sequence of events, it is most likely that deposition of ECM materials is a relatively late phenomenon in the damage sequence, and is not a critical initial step in producing axonal injury. However, in our chronology study, ECM deposition was noted to occur at an early stage, although the pathologic significance of this is still uncertain (Johnson et al., 2000a, b).

Although loss of compliance may not play a direct role in axonal injury, it remains possible that alterations in the physical response of the ONH to changes in IOP could affect axonal susceptibility. Burgoyne and his associates have argued effectively that alterations in the physical characteristics and biomechanical properties of the connective tissues of the optic nerve head can influence the stress and strain forces on these structures produced by changes in IOP (Bellezza et al., 2000). These forces may in turn influence the process of axonal injury, through mechanisms to be discussed below. It is possible that the ECM deposition, by reducing compliance, may significantly alter the physical behavior of the ONH and influence axonal susceptibility to injury. In this manner, these, and other non-axonal changes, could contribute to the progressive nature of glaucomatous injury, resulting in an ever-expanding loss of axons and RGC, even without further increases in IOP.

3.2.2. *Astrocyte responses to elevated IOP*

The cells responsible for producing these ECM changes in pressure-induced optic nerve damage are currently unknown. However, they are likely to be the astrocytes that normally reside within the optic nerve head. Hernandez, working with human glaucoma specimens as well as with organ cultures of optic nerve heads and pure astrocyte cultures, has shown that these cells are capable of responding to varying conditions, including elevated hydrostatic pressure (Pena et al., 2001, 1999; Tezel et al., 2001; Wax et al., 2000). These results include the upregulation of several proteins found to be involved in the optic nerve head response to glaucoma. She has published a thorough description of these astrocyte responses and their potential role in glaucomatous optic nerve damage in a previous issue of this journal. (Hernandez, 2000).

Astrocytes have been shown to react to external changes by undergoing hypertrophy, rounding up and migrating, as well as producing increased amounts of GFAP, a component of glial intermediate filaments. (Varela and Hernandez, 1997) As part of this process, they likely reduce their normal connections to each other and to the connective tissues. We have found that loss of label for connexin-43 within the ONH, a component of gap junctions between astrocytes, is an early response to elevated IOP (Johnson et al., 2000a, b). This would imply that loss of intercellular communication is an early consequence of elevated IOP, and could underlie the loss of cellular organization seen histologically in ONH with elevated IOP. This loss of organization could alter the physical response of this tissue to changes in IOP, and may explain the initial hypercompliance reported by Burgoyne. In addition, astrocyte migration may also produce reduced axonal support, and contribute to further axonal injury.

Another potential category of ONH astrocyte response to elevated IOP is the generation of noxious products that result in injury to the axons. Foremost of these in recent years has been that of nitric oxide. Neufeld, working with glaucomatous human optic nerve heads, noted increased labeling for the enzyme nitric oxide synthase 2 (NOS-2) within the lamina cribrosa region (Neufeld et al., 1997). He hypothesized that production of this enzyme, an inducible form, produces nitric oxide, which is implicated in both excitotoxic and apoptotic forms of cell death. In support of this, he has used the vein cautery model to demonstrate that systemic administration of aminoguanidine, an inhibitor of NOS, significantly reduces the rate of RGC death in response to chronic IOP elevation (Neufeld et al., 1999). Later, this group, working with the same model, found similar protection with a prodrug of *L*-N^6-(iminoethyl)-lysine (SC-51), a more specific inhibitor of NOS-2 (Neufeld et al., 2002).

While this work suggests a potential role of NOS-2 in pressure-induced optic nerve damage, it has not been corroborated in recent studies using other models. In the hypertonic saline model, we were not able to demonstrate reduced axonal injury with aminoguanidine (Morrison et al., 2001). Similarly, McKinnon, using the same model, was not able to show protection with SC-51 (Kasmala et al., 2004). Prompted by these findings, we performed gene array analysis of retinas from animals with elevated IOP and used immunohistochemistry and RTPCR on optic nerve heads and retinas to see if we could detect changes in NOS-2 compared to fellow eyes with normal IOP (Morrison, et al., 2003). We found no evidence of elevation in NOS-2 in any of these evaluations, even though we did find it significantly increased in optic nerve heads of eyes with optic nerve transection. Similarly, John et al., has crossed DBA/2J mice, a genetic glaucoma model, with elevated IOP and well-documented progressive optic nerve damage, with NOS-2 knock-outs (Libby et al., 2003). Although these animals lacked NOS-2 and should have been prevented from developing nerve

damage, there was no attenuation in the injury seen as compared to DBA/2J animals with normal NOS-2 capability. While the pathophysiology of optic nerve damage in this model is not entirely clear, this study strongly suggests that the presence of NOS-2 is not necessary for damage to occur.

Despite these conflicting findings, the nitric oxide synthase theory, and the concept that axonal damage in glaucoma occurs via a damaging substance produced by astrocytes, remains an attractive concept. This is because, as with NOS-2, specific inhibitors do exist which may be potentially useful for testing these theories, and possibly for uncovering a candidate neuroprotective treatment of glaucoma.

However, astrocyte response to changing or elevated IOP may not necessarily damage RGC axons via an active process. Passive processes are also plausible. In this sense, astrocytes responding to changes in elevated IOP may simply cease to perform their normal axonal support functions. One possibility in this category is that of reduced production of neurotrophins. Although neurotrophins that are important to RGC survival originate primarily in the superior colliculus, we have found that astrocytes in the normal rat ONH also label with antibodies to both NT4/5 and BDNF (Johnson et al., 2000a). Following several weeks of elevated IOP, this label disappears, only to reappear at later stages of damage. Currently, it is uncertain if this alteration plays a significant role in axonal injury and RGC death. However, if this change fails to recover following normalization of IOP, this could also contribute to progressive RGC damage in glaucoma.

There are undoubtedly numerous other astrocyte responses that could reduce support for axons. Understanding the normal supportive functions of astrocytes and the consequence of their withdrawal will most likely prove to be a key to understanding the mechanisms of glaucomatous optic nerve damage and the processes that underlie the progressive nature of this injury.

However, any theory requires confirmation by multiple laboratories using several different model systems, including those in primates, before it can be widely accepted. The current availability of the different rat glaucoma models offers a major advantage in this regard. Their reduced cost allows the use of large groups of animals, enabling reasonable statistics to be performed for molecular tissue analysis and drug testing.

4. Effects of elevated IOP on retinal ganglion cells

Elevated IOP produces RGC death, and this is generally felt to be the cause of irreversible vision loss in glaucoma. Understanding the exact mechanisms for this is particularly important for the eventual development of methods to protect RGC or allowing survival of injured RGC that would otherwise die following successful treatment of IOP. Quigley has previously reviewed the potential mechanisms of RGC death in glaucoma. (Quigley, 1999) Using the monkey model of elevated IOP, he demonstrated that most RGC death occurs by apoptosis, an energy-dependent form of cell death distinct from excitotoxic and necrotic death (Quigley et al., 1995). This mode of death occurs by a distinct set of events that is genetically controlled, which opens up many possibilities for intervention.

An intrinsic part of this process is the activation of the caspase family of proteases. This is a regulated series of events involving several members of the family, culminating in the death of the cell. Several investigators have studied this process, and have reported evidence using the hypertonic saline injection model that caspase 3 and 8, and more recently caspase 9, are all elevated in the RGC in response to elevated IOP (Hanninen et al., 2002; McKinnon et al., 2002a). Attempts to exploit these findings could lead to treatments that may prevent or delay the ultimate death of RGC in glaucoma. In fact, McKinnon has used intra-vitreal injection of an adeno-associated viral vector to produce gene expression for baculoviral IOP repeat-containing protein-4 (BIRC4), a caspase inhibitor, in RGC (McKinnon et al., 2002b). When exposed to elevated IOP using the hypertonic saline model, they found that these eyes had significantly less axon loss as compared to eyes injected with normal saline. However, this approach may not address the underlying factors that lead to the activation of this pathway, although it could positively affect the outcome for RGC that are injured but not yet undergoing apoptosis.

4.1. Neurotrophin deprivation and pressure-induced injury

Because of the need to understand early factors that lead to apoptosis in glaucoma, several investigators have focused on the previously mentioned possibility that reduced axonal transport leads to decreased delivery of neurotrophins to the RGC. This delivery is normally accomplished by complexing of BDNF, produced primarily in the superior colliculus, with trkB, originating in the RGC, and the retrograde transport of this complex via retrograde transport to the RGC. In this hypothesis, if neurotrophin delivery is reduced, retinal ganglion cells, which depend on this neurotrophic support for their survival, would ultimately undergo apoptosis and die.

Quigley and his collaborators have documented several steps in this process in rodent models of glaucoma. This includes demonstrating that acutely elevated IOP in cannulated eyes can produce abnormal dilation of RGC axons with accumulations of vesicles within the optic nerve head. By immunohistochemistry,

they found increased labeling for TrkB, behind the optic nerve head, and increased label for both BDNF and TrkB in monkey eyes with chronic glaucoma (Pease et al., 2000). Radiolabeled BDNF injected into the superior colliculus was also found to arrive at the RGC much more slowly in eyes with acutely elevated IOP (Quigley et al., 2000). This same laboratory has recently succeeded in transfecting RGC with an adenoassociated viral vector to cause overexpression of the BDNF gene in the RGC (Martin et al., 2003). When these eyes were exposed to chronically elevated IOP using their limbal laser protocol, they found a significantly reduced loss of RGC axons as compared to eyes without BDNF transfection. This would support the possibility that reduced BDNF delivery contributes to RGC death following elevated IOP. These results, along with the previously discussed transfection study using BIRC4 protein, also offer promise to the potential of gene therapy for glaucoma treatment, and the value of understanding the cellular mechanisms involved. However, as with any observation using animal models, these findings will require independent confirmation.

Using our model, we have tested this neurotrophin theory by immunohistochemistry with antibodies to neurotrophins, their receptors, neurofilament proteins, and proteins involved in cell division and astrocyte communication (Johnson et al., 2000a, b). By assessing labeling for the different proteins in sections from the same eyes, we could determine their coordinated responses in both the retina and the optic nerve head. These were also compared to the timing of retinal ganglion cell damage by analyzing tissues for apoptosis, using the TUNEL method. Animals with elevated IOP over times ranging from 1 day to over 2 months were studied. According to the neurotrophin deprivation hypothesis, we would have expected that, following elevated IOP, obstruction of axonal transport would be observed first, followed by evidence of retinal ganglion cell injury and then axonal loss. Astrocytic responses would be expected to occur concurrent with the axonal changes.

Contrary to predictions of the neurotrophin deprivation hypothesis, we found evidence of retinal ganglion cell apoptosis by TUNEL labeling throughout the time course of this experiment, and not just following axonal transport obstruction. Alterations of neurotrophin distribution to the retina were not detected until later, 1–2 weeks after IOP elevation. These changes appeared as a decrease in label for neurotrophin within the retinal ganglion cell and inner plexiform layers, and were consistent with blockade of retrograde axonal transport. These were also accompanied by apparent obstruction of movement of these proteins across the optic nerve head.

Replacing the supply of neurotrophins to the RGC represents an attractive potential therapy. However, this is a very complex system and neurotrophin supplementation may have unintended consequences. In addition, it is not completely known how elevated IOP affects TrkB production by the RGC. Evidence with our model has shown that chronic IOP elevation results in a reduction in message for Trk B in the retina (Jia et al., 2004). This reduction, or its failure to return to normal following reduction of IOP after a moderate amount of damage, could present other potential treatment opportunities for patients with advanced glaucoma.

4.2. RGC changes prior to cell death

Another important factor that may contribute to progressive damage in glaucoma is the possibility that RGC faced with elevated IOP may undergo a gradual reduction in their structure and function, prior to death. Weber has noted that, in experimental primate glaucoma, RGC undergo reduction in the size of their dendritic arborization, followed by reduction in the size of the cell bodies and axons (Weber et al., 1998). This would suggest that there may indeed be an opportunity for rescue of these cells that are undergoing injury, but possibly not yet committed to die. We have also noted that reduction in neurofilament production is a common feature in RGC exposed to chronic IOP elevation (Johnson et al., 2000b). This presents as a graded response, increasing with more extensive optic nerve damage. Message for alpha-tubulin, produced primarily by RGC, does not appear to change in this system, suggesting that such changes are relatively selective. A similar decrease, well in advance of the loss of RGC, has also been observed for Thy-1 message production, an axonal marker for RGC (Schlamp et al., 2001).

From these findings, it appears that RGC undergo specific cellular changes during the glaucomatous process. While these changes likely precede the death of the RGC, it is not currently clear whether or not they can be reversed by simply lowering eye pressure. If not, such reductions in cellular activity could contribute significantly to the progressive nature of vision loss in glaucoma. Devising ways to induce such a reversal could represent an effective potential approach to neuroprotection.

4.3. Heat shock proteins

An additional effect of elevated IOP on RGC includes activation of heat shock proteins. These proteins, induced by exposure to heat or other forms of metabolic stress, have been found to provide a protective role for neural tissue with ischemic insults and in retinas exposed to light-induced toxicity. Using the laser-India ink model in rats, Park found an early increase in retinal Hsp72, that later decreased to baseline (Park et al., 2001). However, they found that parenteral administra-

tion of zinc induced a strong Hsp72 response. They also noted that this, as well as treatment with hyperthermia (a heat stress), reduced RGC death in their model of pressure elevation. In a follow-up study, they found that administration of geranylgeralylacetone, a heat shock protein-inducing agent, increased expression of Hsp72 in RGC (Ishii et al., 2003). They found that this agent, too, reduced loss of RGC in their model. This represents an attractive approach to neuroprotection, since it would be accomplished by enhancing endogenous mechanisms already present within the animal. However, RGC do not appear to maintain the ability, on their own, to enhance this effect in the face of elevated IOP.

4.4. Glutamate toxicity

Glutamate toxicity is another potential mechanism of RGC loss in glaucoma that has received considerable attention over the years. This was prompted by the discovery of elevated levels of glutamate, an excitatory neurotransmitter, in the vitreous of human glaucomatous eyes and in monkeys with experimental glaucoma (Dreyer et al., 1996). In addition, glutamate injected into the vitreous can produce selective damage to RGC (Vorwerk et al., 1996). These investigators hypothesized that elevated glutamate levels were responsible for the RGC damage in glaucoma, through an excitotoxic mechanism. Possibly, this increase resulted from reduced function of glutamate transporters in retinal glial cells responsible for the reuptake of released glutamate into the cell.

However, more recent investigations in humans (Honkanen et al., 2003) and monkeys (Carter-Dawson et al., 2002) have provided conflicting evidence. In rats, too, neither chronic elevation of IOP nor optic nerve transection was found to produce a specific increase in intravitreal glutamate (Levkovitch-Verbin et al., 2002a), although increased levels of amino acids were noted. On the other hand, reduced presence of glutamate transporters were noted in a separate study in both types of optic nerve injury (Martin et al., 2002). At present, the precise role of glutamate toxicity in glaucoma or pressure-induced optic nerve damage remains controversial, requiring further study with these models. Regardless of the outcome, these prospects illustrate the importance of evaluating retinal glial responses to elevated IOP. Augmenting or reversing these responses may result in neuroprotective treatments for partially damaged RGC in glaucoma.

5. Future directions

It is clear that chronic pressure-induced optic nerve damage involves cellular changes in both the optic nerve head and retina. Alterations in one or both regions could conceivably contribute to the progressive nature of vision loss that is characteristic of glaucoma. Such changes, if found to be not reversible following subsequent control of IOP, may also help explain the phenomenon of heightened susceptibility of the glaucomatous eye, even following ''successful'' conventional glaucoma management. This could explain progressive deterioration of visual function in patients with ''normal tension glaucoma'' and in patients with ''end-stage'' disease, who continue to lose vision in spite of aggressive pressure control (Grant and Burke, 1982).

From this standpoint, one area that must be developed is a model that mimics the phenomenon of partial optic nerve damage, wherein IOP is elevated for a given period of time and then reliably lowered to the normal range (Cepurna, et al., 2003). The laser model, which has been reported to provide a limited duration of IOP elevation, may also prove useful in this regard (Levkovitch-Verbin et al., 2002b). Using such a paradigm would provide insights into the ability of partially damaged RGC to either recover or suffer progressive loss. Understanding the nature of the cellular response to this situation and the specific functions that are not restored would provide useful insights into potential new therapies to rescue partially damaged RGC and their axons.

This understanding will be equally important for injury occurring in the optic nerve head. It is clear that loss of the normal architecture of the optic nerve head, including loss of axons, astrocyte migration and posterior bowing of the supporting tissues, is a characteristic of this disease. While it is unlikely that normal architecture is restored following pressure lowering, the response of individual cells within the nerve head to pressure lowering is totally unknown.

Another factor that will be extremely important for bringing us closer to understanding the nature of progressive glaucomatous vision loss is the aging process as it affects both the retina and optic nerve. Glaucoma is well recognized as more common in the elderly. With the growing numbers of elderly people in the industrialized nations, the interaction of glaucoma and elevated IOP on the aging eye will become increasingly important. Aging changes may contribute significantly to the progressive nature of glaucomatous vision loss.

Currently, little beyond histologic descriptions of axonal changes is known about aging. Light and electron microscopic analyses of the optic nerve in monkeys, humans and rats indicate that axonal numbers are lost with age (Morrison et al., 1990a; Repka and Quigley, 1989; Ricci et al., 1988; Sandell and Peters, 2001). However, alterations in numerous cellular activities of RGC and the cells of the ONH are simply unknown. These would include neurotrophin and their receptor changes, as well as functions directed at

maintenance of the axon, such as neurofilament proteins. Clearly, gradual reductions in these crucial functions would have a significant impact on the response of the retina and ONH to elevated pressure, as well as on their ability to recover from a period of elevated pressure following its normalization.

Finally, better understanding of the normal functions of cells within the optic nerve head, including astrocyte support to axons, is needed. We also need a more complete understanding of cellular responses within the optic nerve head, in addition to those described here, and how they contribute to axonal damage in glaucoma.

Fortunately, many of the tools needed for identifying and understanding these alterations are now available. Reliable models of chronically elevated IOP exist, as well as methods to monitor the IOP and quantify the resulting optic nerve and retinal damage. These can be applied to tissue analyses, such as immunohistochemistry, for correlation with observations of human glaucoma specimens. In addition, the favorable expense of the rodent models allow detailed analyses of cellular and molecular responses, and provide opportunities for genetic manipulations as well as in vivo testing of potential neuroprotective agents.

Acknowledgements

Work supported in part by National Institutes of Health Grant #R01-10145 (NEI) and unrestricted funds from Research to Prevent Blindness. Dr. Morrison is a 2001 Lew Wasserman RPB Scholar.

References

The Advanced Glaucoma Intervention Study (AGIS), 2000. 7. The relationship between control of intraocular pressure and visual field deterioration The AGIS Investigators. Am. J. Ophthalmol. 130, 429–440.

Ahmed, F.A., Hegazy, K., Chaudhary, P., Sharma, S.C., 2001. Neuroprotective effect of alpha(2) agonist (brimonidine) on adult rat retinal ganglion cells after increased intraocular pressure. Brain Res. 913, 133–139.

Anderson, D.R., 1969. Ultrastructure of human and monkey lamina cribrosa and optic nerve head. Arch. Ophthalmol. 82, 800–814.

Anderson, D.R., 1970. Ultrastructure of the optic nerve head. Arch. Ophthalmol. 83, 63–73.

Anderson, D.R., Hendrickson, A., 1974. Effect of intraocular pressure on rapid axoplasmic transport in monkey optic nerve. Invest. Ophthalmol. 13, 771–783.

Archibald, M.L., Le Vatte, T., Chauhan, B.C., 2003. Semi-Quantitative Method for Grading Optic Nerve Damage in Rats. Invest. Ophthalmol. Vis. Sci. 44, E Abstract 3346.

Asrani, S., Zeimer, R., Wilensky, J., Gieser, D., Vitale, S., Lindenmuth, K., 2000. Large diurnal fluctuations in intraocular pressure are an independent risk factor in patients with glaucoma. J. Glaucoma 9, 134–142.

Bakalash, S., Kipnis, J., Yoles, E., Schwartz, M., 2002. Resistance of retinal ganglion cells to an increase in intraocular pressure is immune-dependent. Invest. Ophthalmol. Vis. Sci. 43, 2648–2653.

Bayer, A.U., Danias, J., Brodie, S., Maag, K.P., Chen, B., Shen, F., Podos, S.M., Mittag, T.W., 2001. Electroretinographic abnormalities in a rat glaucoma model with chronic elevated intraocular pressure. Exp. Eye Res. 72, 667–677.

Bellezza, A.J., Hart, R.T., Burgoyne, C.F., 2000. The optic nerve head as a biomechanical structure: initial finite element modeling. Invest. Ophthalmol. Vis. Sci. 41, 2991–3000.

Bellezza, A.J., Rintalan, C.J., Thompson, H.W., Downs, J.C., Hart, R.T., Burgoyne, C.F., 2003. Deformation of the lamina cribrosa and anterior scleral canal wall in early experimental glaucoma. Invest. Ophthalmol. Vis. Sci. 44, 623–637.

Burgoyne, C.F., Quigley, H.A., Thompson, H.W., Vitale, S., Varma, R., 1995a. Early changes in optic disc compliance and surface position in experimental glaucoma. Ophthalmology 102, 1800–1809.

Burgoyne, C.F., Quigley, H.A., Thompson, H.W., Vitale, S., Varma, R., 1995b. Measurement of optic disc compliance by digitized image analysis in the normal monkey eye. Ophthalmology 102, 1790–1799.

Burgoyne, C.F., Mercante, D.E., Thompson, H.W., 2002. Change detection in regional and volumetric disc parameters using longitudinal confocal scanning laser tomography. Ophthalmology 109, 455–466.

Carter-Dawson, L., Crawford, M.L., Harwerth, R.S., Smith III., E.L., Feldman, R., Shen, F.F., Mitchell, C.K., Whitetree, A., 2002. Vitreal glutamate concentration in monkeys with experimental glaucoma. Invest. Ophthalmol. Vis. Sci. 43, 2633–2637.

Cepurna, W.O., Jia, L., Barber, S.L., Johnson, E.C., Morrison, J.C., 2003. Use of Cyclodialysis to Control Intraocular Pressure Elevation in Brown Norway Rats With Experimental Glaucoma. Invest. Ophthalmolol. Vis. Sci. 44 E Abstract 3328.

Chauhan, B.C., Pan, J., Archibald, M.L., LeVatte, T.L., Kelly, M.E., Tremblay, F., 2002. Effect of intraocular pressure on optic disc topography, electroretinography, and axonal loss in a chronic pressure-induced rat model of optic nerve damage. Invest. Ophthalmol. Vis. Sci. 43, 2969–2976.

Cioffi, G.A., Van Buskirk, E.M., 1994. Microvasculature of the anterior optic nerve. Surv. Ophthalmol. 38 (Suppl.), S107–S116 discussion S116-107.

Cohan, B.E., Bohr, D.F., 2001a. Goldmann applanation tonometry in the conscious rat. Invest. Ophthalmol. Vis. Sci. 42, 340–342.

Cohan, B.E., Bohr, D.F., 2001b. Measurement of intraocular pressure in awake mice. Invest. Ophthalmol. Vis. Sci. 42, 2560–2562.

Danias, J., Shen, F., Goldblum, D., Chen, B., Ramos-Esteban, J., Podos, S.M., Mittag, T., 2002. Cytoarchitecture of the retinal ganglion cells in the rat. Invest. Ophthalmol. Vis. Sci. 43, 587–594.

Drance, S.M., 1999. The Collaborative Normal-Tension Glaucoma Study and some of its lessons. Can. J. Ophthalmol. 34, 1–6.

Dreyer, E.B., Zurakowski, D., Schumer, R.A., Podos, S.M., Lipton, S.A., 1996. Elevated glutamate levels in the vitreous body of humans and monkeys with glaucoma. Arch. Ophthalmol. 114, 299–305.

Erickson-Lamy, K.A., Kaufman, P.L., McDermott, M.L., France, N.K., 1984. Comparative anesthetic effects on aqueous humor dynamics in the cynomolgus monkey. Arch. Ophthalmol. 102, 1815–1820.

Frishman, L.J., Saszik, S., Harwerth, R.S., Viswanathan, S., Li, Y., Smith III., E.L., Robson, J.G., Barnes, G., 2000. Effects of experimental glaucoma in macaques on the multifocal ERG. Multifocal ERG in laser-induced glaucoma. Doc. Ophthalmol. 100, 231–251.

Gaasterland, D., Tanishima, T., Kuwabara, T., 1978. Axoplasmic flow during chronic experimental glaucoma. 1. Light and electron

microscopic studies of the monkey optic nervehead during development of glaucomatous cupping. Invest. Ophthalmol. Vis. Sci. 17, 838–846.

Gaasterland, D., Kupfer, C., 1974. Experimental glaucoma in the rhesus monkey. Invest. Ophthalmol. 13, 455–457.

Glovinsky, Y., Quigley, H.A., Dunkelberger, G.R., 1991. Retinal ganglion cell loss is size dependent in experimental glaucoma. Invest. Ophthalmol Vis Sci 32, 484–491.

Goldblum, D., Mittag, T., 2002. Prospects for relevant glaucoma models with retinal ganglion cell damage in the rodent eye. Vision Res. 42, 471–478.

Goldblum, D., Kontiola, A.I., Mittag, T., Chen, B., Danias, J., 2002. Non-invasive determination of intraocular pressure in the rat eye. Comparison of an electronic tonometer (TonoPen), and a rebound (impact probe) tonometer. Graefes Arch. Clin. Exp. Ophthalmol. 240, 942–946.

Grant, W.M., Burke Jr., J.F., 1982. Why do some people go blind from glaucoma? Ophthalmology 89, 991–998.

Gregory, D.S., Aviado, D.G., Sears, M.L., 1985. Cervical ganglionectomy alters the circadian rhythm of intraocular pressure in New Zealand White rabbits. Curr. Eye Res. 4, 1273–1279.

Grozdanic, S.D., Betts, D.M., Sakaguchi, D.S., Allbaugh, R.A., Kwon, Y.H., Kardon, R.H., 2003a. Laser-induced mouse model of chronic ocular hypertension. Invest. Ophthalmol. Vis. Sci. 44, 4337–4346.

Grozdanic, S.D., Betts, D.M., Sakaguchi, D.S., Kwon, Y.H., Kardon, R.H., Sonea, I.M., 2003b. Temporary elevation of the intraocular pressure by cauterization of vortex and episcleral veins in rats causes functional deficits in the retina and optic nerve. Exp. Eye Res. 77, 27–33.

Hanninen, V.A., Pantcheva, M.B., Freeman, E.E., Poulin, N.R., Grosskreutz, C.L., 2002. Activation of caspase 9 in a rat model of experimental glaucoma. Curr. Eye Res. 25, 389–395.

Harwerth, R.S., Smith III., E.L., Chandler, M., 1999. Progressive visual field defects from experimental glaucoma: measurements with white and colored stimuli. Optim. Vis. Sci. 76, 558–570.

Harwerth, R.S., Crawford, M.L., Frishman, L.J., Viswanathan, S., Smith III., E.L., Carter-Dawson, L., 2002. Visual field defects and neural losses from experimental glaucoma. Prog. Retin. Eye Res. 21, 91–125.

Heickell, A.G., Bellezza, A.J., Thompson, H.W., Burgoyne, C.F., 2001. Optic disc surface compliance testing using confocal scanning laser tomography in the normal monkey eye. J. Glaucoma 10, 369–382.

Hernandez, M.R., 1992. Ultrastructural immunocytochemical analysis of elastin in the human lamina cribrosa. Changes in elastic fibers in primary open-angle glaucoma. Invest. Ophthalmol. Vis. Sci. 33, 2891–2903.

Hernandez, M.R., 2000. The optic nerve head in glaucoma: role of astrocytes in tissue remodeling. Prog. Retin. Eye Res. 19, 297–321.

Hernandez, M.R., Luo, X.X., Igoe, F., Neufeld, A.H., 1987. Extracellular matrix of the human lamina cribrosa. Am. J. Ophthalmol. 104, 567–576.

Hernandez, M.R., Andrzejewska, W.M., Neufeld, A.H., 1990. Changes in the extracellular matrix of the human optic nerve head in primary open-angle glaucoma. Am. J. Ophthalmol. 109, 180–188.

Honkanen, R.A., Baruah, S., Zimmerman, M.B., Khanna, C.L., Weaver, Y.K., Narkiewicz, J., Waziri, R., Gehrs, K.M., Weingeist, T.A., Boldt, H.C., Folk, J.C., Russell, S.R., Kwon, Y.H., 2003. Vitreous amino acid concentrations in patients with glaucoma undergoing vitrectomy. Arch. Ophthalmol. 121, 183–188.

Ishii, Y., Kwong, J.M., Caprioli, J., 2003. Retinal ganglion cell protection with geranylgeranylacetone, a heat shock protein inducer, in a rat glaucoma model. Invest. Ophthalmol. Vis. Sci. 44, 1982–1992.

Jia, L., Cepurna, W.O., Johnson, E.C., Morrison, J.C., 2000a. Effect of general anesthetics on IOP in rats with experimental aqueous outflow obstruction. Invest. Ophthalmol. Vis. Sci. 41, 3415–3419.

Jia, L., Cepurna, W.O., Johnson, E.C., Morrison, J.C., 2000b. Patterns of intraocular pressure elevation after aqueous humor outflow obstruction in rats. Invest. Ophthalmol. Vis. Sci. 41, 1380–1385.

Jia, L., W.O.C., Barber, S.L., Morrison, J.C., Johnson, E.C., 2004. Retinal Neurotrophin And Trk Receptor mRNA Expression Following Elevated Intraocular Pressure Or Optic Nerve Transection. Invest. Ophthalmol. Vis. Sci. 45.

Johnson, E.C., Morrison, J.C., Farrell, S., Deppmeier, L., Moore, C.G., McGinty, M.R., 1996. The effect of chronically elevated intraocular pressure on the rat optic nerve head extracellular matrix. Exp. Eye Res. 62, 663–674.

Johnson, E.C., Deppmeier, L.M., Wentzien, S.K., Hsu, I., Morrison, J.C., 2000a. Chronology of optic nerve head and retinal responses to elevated intraocular pressure. Invest. Ophthalmol. Vis. Sci. 41, 431–442.

Johnson, E.J.L., Cepurna, W.O., Ackhavong, V., Morrison, J.C., 2000b. Elevated intraocular pressure affects the levels of neurofilament mRNA in the retina. Invest. Ophthalmol. Vis. Sci. (suppl) 41, S4764.

Kasmala L.T., Ransom, N.L., Conner, J.R., McKinnon, S. J., 2004. Oral administration of SC-51, a nitric oxide synthase inhibitor, does not protect opotic nerve axons in a hypertensive rat model of glaucoma. Invest. Ophthalmol. Vis. Sci., EAbstract 904.

Kass, M.A., Heuer, D.K., Higginbotham, E.J., Johnson, C.A., Keltner, J.L., Miller, J.P., Parrish, IIR.K., Wilson, M.R., Gordon, M.O., 2002. The ocular hypertension treatment study: a randomized trial determines that topical ocular hypotensive medication delays or prevents the onset of primary open-angle glaucoma. Arch. Ophthalmol. 120, 701–713 discussion 829-730.

Kaufman, P.L., Davis, G.E., 1980. ''Minified'' Goldmann applanating prism for tonometry in monkeys and humans. Arch. Ophthalmol. 98, 542–546.

Kerrigan-Baumrind, L.A., Quigley, H.A., Pease, M.E., Kerrigan, D.F., Mitchell, R.S., 2000. Number of ganglion cells in glaucoma eyes compared with threshold visual field tests in the same persons. Invest. Ophthalmol. Vis. Sci. 41, 741–748.

Ko, M.L., Hu, D.N., Ritch, R., Sharma, S.C., Chen, C.F., 2001. Patterns of retinal ganglion cell survival after brain-derived neurotrophic factor administration in hypertensive eyes of rats. Neurosci. Lett. 305, 139–142.

Konstas, A.G., Mantziris, D.A., Stewart, W.C., 1997. Diurnal intraocular pressure in untreated exfoliation and primary open-angle glaucoma. Arch. Ophthalmol. 115, 182–185.

Kontiola, A.I., Goldblum, D., Mittag, T., Danias, J., 2001. The induction/impact tonometer: a new instrument to measure intraocular pressure in the rat. Exp. Eye Res. 73, 781–785.

LaVail, M.M., 1980. Eye pigmentation and constant light damage in the rat retina. In: Williams, T.P., Baker, B.N. (Eds.), The Effects of constant light on visual processes. Plenum Press, New York, pp. 357–387.

LaVail, M.M., Matthes, M.T., Yasumura, D., Faktorovich, E.G., Steinberg, R.H., 1997. Histological Method to Assess Photoreceptor Light Damage and Protection by Survival Factors. Plenum Press, New York.

Leske, M.C., Heijl, A., Hussein, M., Bengtsson, B., Hyman, L., Komaroff, E., 2003. Factors for glaucoma progression and the effect of treatment: the early manifest glaucoma trial. Arch. Ophthalmol. 121, 48–56.

Levkovitch-Verbin, H., Martin, K.R., Quigley, H.A., Baumrind, L.A., Pease, M.E., Valenta, D., 2002a. Measurement of amino acid levels in the vitreous humor of rats after chronic intraocular pressure elevation or optic nerve transection. J. Glaucoma 11, 396–405.

Levkovitch-Verbin, H., Quigley, H.A., Martin, K.R., Valenta, D., Baumrind, L.A., Pease, M.E., 2002b. Translimbal laser photocoagulation to the trabecular meshwork as a model of glaucoma in rats. Invest. Ophthalmol. Vis. Sci. 43, 402–410.

Libby R.T., Smith, R.S., Savinova, O.V., Clark, A.F., John, S.W.M., 2003. Inducible nitric oxide synthase (Nos2) is not required for glaucomaotus optic nerve damage in DBA/2J mice. Invest. Ophthalmol. Vis. Sci. 44, EAbstract #145.

Martin, K.R., Levkovitch-Verbin, H., Valenta, D., Baumrind, L., Pease, M.E., Quigley, H.A., 2002. Retinal glutamate transporter changes in experimental glaucoma and after optic nerve transection in the rat. Invest. Ophthalmol. Vis. Sci. 43, 2236–2243.

Martin, K.R., Quigley, H.A., Zack, D.J., Levkovitch-Verbin, H., Kielczewski, J., Valenta, D., Baumrind, L., Pease, M.E., Klein, R.L., Hauswirth, W.W., 2003. Gene therapy with brain-derived neurotrophic factor as a protection: retinal ganglion cells in a rat glaucoma model. Invest. Ophthalmol. Vis. Sci. 44, 4357–4365.

McKinnon, S.J., Lehman, D.M., Kerrigan-Baumrind, L.A., Merges, C.A., Pease, M.E., Kerrigan, D.F., Ransom, N.L., Tahzib, N.G., Reitsamer, H.A., Levkovitch-Verbin, H., Quigley, H.A., Zack, D.J., 2002a. Caspase activation and amyloid precursor protein cleavage in rat ocular hypertension. Invest. Ophthalmol. Vis. Sci. 43, 1077–1087.

McKinnon, S.J., Lehman, D.M., Tahzib, N.G., Ransom, N.L., Reitsamer, H.A., Liston, P., LaCasse, E., Li, Q., Korneluk, R.G., Hauswirth, W.W., 2002b. Baculoviral IAP Repeat-Containing-4 Protects Optic Nerve Axons in a Rat Glaucoma Model. Mol. Ther. 5, 780–787.

McLaren, J.W., Brubaker, R.F., FitzSimon, J.S., 1996. Continuous measurement of intraocular pressure in rabbits by telemetry. Invest. Ophthalmol. Vis. Sci. 37, 966–975.

Minckler, D.S., Bunt, A.H., Johanson, G.W., 1977. Orthograde and retrograde axoplasmic transport during acute ocular hypertension in the monkey. Invest. Ophthalmol. Vis. Sci. 16, 426–441.

Mittag, T.W., Danias, J., Pohorenec, G., Yuan, H.M., Burakgazi, E., Chalmers-Redman, R., Podos, S.M., Tatton, W.G., 2000. Retinal damage after 3 to 4 months of elevated intraocular pressure in a rat glaucoma model. Invest. Ophthalmol. Vis. Sci. 41, 3451–3459.

Moore, C.G., Milne, S.T., Morrison, J.C., 1993. Noninvasive measurement of rat intraocular pressure with the Tono-Pen. Invest. Ophthalmol. Vis. Sci. 34, 363–369.

Moore, C.G., Epley, D., Milne, S.T., Morrison, J.C., 1995. Long-term non-invasive measurement of intraocular pressure in the rat eye. Curr. Eye Res. 14, 711–717.

Moore, C.G., Johnson, E.C., Morrison, J.C., 1996. Circadian rhythm of intraocular pressure in the rat. Curr. Eye Res. 15, 185–191.

Morrison, J.C., DeFrank, M.P., Van Buskirk, E.M., 1987. Comparative microvascular anatomy of mammalian ciliary processes. Invest. Ophthalmol. Vis. Sci. 28, 1325–1340.

Morrison, J.C., Jerdan, J.A., L'Hernault, N.L., Quigley, H.A., 1988. The extracellular matrix composition of the monkey optic nerve head. Invest. Ophthalmol. Vis. Sci. 29, 1141–1150.

Morrison, J.C., L'Hernault, N.L., Jerdan, J.A., Quigley, H.A., 1989. Ultrastructural location of extracellular matrix components in the optic nerve head. Arch. Ophthalmol. 107, 123–129.

Morrison, J.C., Cork, L.C., Dunkelberger, G.R., Brown, A., Quigley, H.A., 1990a. Aging changes of the rhesus monkey optic nerve. Invest. Ophthalmol. Vis. Sci. 31, 1623–1627.

Morrison, J.C., Dorman-Pease, M.E., Dunkelberger, G.R., Quigley, H.A., 1990b. Optic nerve head extracellular matrix in primary optic atrophy and experimental glaucoma. Arch. Ophthalmol. 108, 1020–1024.

Morrison, J.C., Rask, P., Johnson, E.C., Deppmeier, L., 1994. Chondroitin sulfate proteoglycan distribution in the primate optic nerve head. Invest. Ophthalmol. Vis. Sci. 35, 838–845.

Morrison, J., Farrell, S., Johnson, E., Deppmeier, L., Moore, C.G., Grossmann, E., 1995a. Structure and composition of the rodent lamina cribrosa. Exp. Eye Res. 60, 127–135.

Morrison, J.C., Fraunfelder, F.W., Milne, S.T., Moore, C.G., 1995b. Limbal microvasculature of the rat eye. Invest. Ophthalmol. Vis. Sci. 36, 751–756.

Morrison, J.C., Johnson, E.C., Funk, R., 1997a. Microvasculature of the rat optic nerve head (ARVO). Invest. Ophthalmol. Vis. Sci. 38, S273.

Morrison, J.C., Moore, C.G., Deppmeier, L.M., Gold, B.G., Meshul, C.K., Johnson, E.C., 1997b. A rat model of chronic pressure-induced optic nerve damage. Exp. Eye Res. 64, 85–96.

Morrison, J.C., Johnson, E.C., Cepurna, W., 1998. Animal models in glaucoma research. Ophthalmic Practice 16, 12–20.

Morrison, J.C., Cepurna, W.O., Johnson, E.C., 1999a. Modeling glaucomatous optic nerve damage. Int. Ophthalmol. Clin. 39, 29–41.

Morrison, J.C., Johnson, E.C., Cepurna, W.O., Funk, R.H., 1999b. Microvasculature of the rat optic nerve head. Invest. Ophthalmol. Vis. Sci. 40, 1702–1709.

Morrison, J.C., Johnson, E.C., Jia, L., Cepurna, W.O., 2001. Effect of aminoguanidine on optic nerve injury following intraocular pressure elevation in the rat. Invest. Ophthalmol. Vis. Sci. 42, S413.

Morrison, J.C., Cepurna, W.O., Jia, L., Aubert, J., Johnson, E.C., 2002. Mechanism of focal optic nerve injury from elevated intraocular pressure. IOVS Abstract #2885.

Morrison, J.C., Johnson, E.C., Shepard, A.R., Cepurna, W.O., Clark, A.F., 2003. Inducible nitric oxide synthase (iNOS) in a rat glaucoma model with chronic elevated intraocular pressure resulting from aqueous humor outflow obstruction. Invest. Ophthalmol. Vis. Sci. 44, Abstract #2101.

Neufeld, A.H., Hernandez, M.R., Gonzalez, M., 1997. Nitric oxide synthase in the human glaucomatous optic nerve head. Arch. Ophthalmol. 115, 497–503.

Neufeld, A.H., Sawada, A., Becker, B., 1999. Inhibition of nitric-oxide synthase 2 by aminoguanidine provides neuroprotection of retinal ganglion cells in a rat model of chronic glaucoma. Proc. Natl. Acad. Sci. USA 96, 9944–9948.

Neufeld, A.H., Das, S., Vora, S., Gachie, E., Kawai, S., Manning, P.T., Connor, J.R., 2002. A prodrug of a selective inhibitor of inducible nitric oxide synthase is neuroprotective in the rat model of glaucoma. J. Glaucoma 11, 221–225.

Nork, T.M., VerHoeve, J.N., Poulsen, G.L., Nickells, R.W., Davis, M.D., Weber, A.J., Vaegan, Sarks, S.H., Lemley, H.L., Millecchia, L.L., 2000. Swelling and loss of photoreceptors in chronic human and experimental glaucomas. Arch. Ophthalmol. 118, 235–245.

Park, K.H., Cozier, F., Ong, O.C., Caprioli, J., 2001. Induction of heat shock protein 72 protects retinal ganglion cells in a rat glaucoma model. Invest. Ophthalmol. Vis. Sci. 42, 1522–1530.

Pease, M.E., McKinnon, S.J., Quigley, H.A., Kerrigan-Baumrind, L.A., Zack, D.J., 2000. Obstructed axonal transport of BDNF and its receptor TrkB in experimental glaucoma. Invest. Ophthalmol. Vis. Sci. 41, 764–774.

Pena, J.D., Varela, H.J., Ricard, C.S., Hernandez, M.R., 1999. Enhanced tenascin expression associated with reactive astrocytes in human optic nerve heads with primary open angle glaucoma. Exp. Eye Res. 68, 29–40.

Peterson, J.A., Kiland, J.A., Croft, M.A., Kaufman, P.L., 1996. Intraocular pressure measurement in cynomolgus monkeys. Tono-Pen versus manometry. Invest. Ophthalmol. Vis. Sci. 37, 1197–1199.

Pena, J.D., Agapova, O., Gabelt, B.T., Levin, L.A., Lucarelli, M.J., Kaufman, P.L., Hernandez, M.R., 2001. Increased elastin expression in astrocytes of the lamina cribrosa in response to elevated intraocular pressure. Invest. Ophthalmol. Vis. Sci. 42, 2303–2314.

Quigley, H.A., 1986. Examination of the retinal nerve fiber layer in the recognition of early glaucoma damage. Trans. Am. Ophthalmol. Soc. 84, 920–966.

Quigley, H.A., 1995. Ganglion cell death in glaucoma: pathology recapitulates ontogeny. Aust. NZ J. Ophthalmol. 23, 85–91.

Quigley, H.A., 1999. Neuronal death in glaucoma. Prog. Retin. Eye Res. 18, 39–57.

Quigley, H.A., 2001. Selective citation of evidence regarding photoreceptor loss in glaucoma. Arch. Ophthalmol. 119, 1390–1391.

Quigley, H.A., Addicks, E.M., 1980. Chronic experimental glaucoma in primates. I. Production of elevated intraocular pressure by anterior chamber injection of autologous ghost red blood cells. Invest. Ophthalmol. Vis. Sci. 19, 126–136.

Quigley, H., Anderson, D.R., 1976. The dynamics and location of axonal transport blockade by acute intraocular pressure elevation in primate optic nerve. Invest. Ophthalmol. 15, 606–616.

Quigley, H.A., Anderson, D.R., 1977. Distribution of axonal transport blockade by acute intraocular pressure elevation in the primate optic nerve head. Invest. Ophthalmol. Vis. Sci. 16, 640–644.

Quigley, H.A., Green, W.R., 1979. The histology of human glaucoma cupping and optic nerve damage: clinicopathologic correlation in 21 eyes. Ophthalmology 86, 1803–1830.

Quigley, H.A., Hohman, R.M., 1983. Laser energy levels for trabecular meshwork damage in the primate eye. Invest. Ophthalmol. Vis. Sci. 24, 1305–1307.

Quigley, H.A., Addicks, E.M., Green, W.R., Maumenee, A.E., 1981. Optic nerve damage in human glaucoma. II. The site of injury and susceptibility to damage. Arch. Ophthalmol. 99, 635–649.

Quigley, H.A., Hohman, R.M., Addicks, E.M., Massof, R.W., Green, W.R., 1983. Morphologic changes in the lamina cribrosa correlated with neural loss in open-angle glaucoma. Am. J. Ophthalmol. 95, 673–691.

Quigley, H.A., Sanchez, R.M., Dunkelberger, G.R., L'Hernault, N.L., Baginski, T.A., 1987. Chronic glaucoma selectively damages large optic nerve fibers. Invest. Ophthalmol. Vis. Sci. 28, 913–920.

Quigley, H.A., Dunkelberger, G.R., Green, W.R., 1988. Chronic human glaucoma causing selectively greater loss of large optic nerve fibers. Ophthalmology 95, 357–363.

Quigley, H.A., Dunkelberger, G.R., Green, W.R., 1989. Retinal ganglion cell atrophy correlated with automated perimetry in human eyes with glaucoma. Am. J. Ophthalmol. 107, 453–464.

Quigley, H.A., Brown, A., Dorman-Pease, M.E., 1991. Alterations in elastin of the optic nerve head in human and experimental glaucoma. Br. J. Ophthalmol. 75, 552–557.

Quigley, H.A., Nickells, R.W., Kerrigan, L.A., Pease, M.E., Thibault, D.J., Zack, D.J., 1995. Retinal ganglion cell death in experimental glaucoma and after axotomy occurs by apoptosis. Invest. Ophthalmol. Vis. Sci. 36, 774–786.

Quigley, H.A., McKinnon, S.J., Zack, D.J., Pease, M.E., Kerrigan-Baumrind, L.A., Kerrigan, D.F., Mitchell, R.S., 2000. Retrograde axonal transport of BDNF in retinal ganglion cells is blocked by acute IOP elevation in rats. Invest. Ophthalmol. Vis. Sci. 41, 3460–3466.

Repka, M.X., Quigley, H.A., 1989. The effect of age on normal human optic nerve fiber number and diameter. Ophthalmology 96, 26–32.

Ricci, A., Bronzetti, E., Amenta, F., 1988. Effect of ageing on the nerve fibre population of rat optic nerve. Gerontology 34, 231–235.

Rowland, J.M., Potter, D.E., Reiter, R.J., 1981. Circadian rhythm in intraocular pressure a rabbit model. Curr. Eye Res. 1, 169–173.

Sandell, J.H., Peters, A., 2001. Effects of age on nerve fibers in the rhesus monkey optic nerve. J. Comp. Neurol. 429, 541–553.

Sawada, A., Neufeld, A.H., 1999. Confirmation of the rat model of chronic, moderately elevated intraocular pressure. Exp. Eye Res. 69, 525–531.

Schlamp, C.L., Johnson, E.C., Li, Y., Morrison, J.C., Nickells, R.W., 2001. Changes in Thy1 gene expression associated with damaged retinal ganglion cells. Mol. Vis. 7, 192–201.

Schori, H., Kipnis, J., Yoles, E., WoldeMussie, E., Ruiz, G., Wheeler, L.A., Schwartz, M., 2001. Vaccination for protection of retinal ganglion cells against death from glutamate cytotoxicity and ocular hypertension: implications for glaucoma. Proc. Natl. Acad. Sci. USA 98, 3398–3403.

Shareef, S.R., Garcia-Valenzuela, E., Salierno, A., Walsh, J., Sharma, S.C., 1995. Chronic ocular hypertension following episcleral venous occlusion in rats [letter]. Exp. Eye Res. 61, 379–382.

Sommer, A., Katz, J., Quigley, H.A., Miller, N.R., Robin, A.L., Richter, R.C., Witt, K.A., 1991. Clinically detectable nerve fiber atrophy precedes the onset of glaucomatous field loss. Arch. Ophthalmol. 109, 77–83.

Sugiyama, K., Gu, Z.B., Kawase, C., Yamamoto, T., Kitazawa, Y., 1999. Optic nerve and peripapillary choroidal microvasculature of the rat eye. Invest. Ophthalmol. Vis. Sci. 40, 3084–3090.

Tezel, G., Hernandez, M.R., Wax, M.B., 2001. In vitro evaluation of reactive astrocyte migration, a component of tissue remodeling in glaucomatous optic nerve head. Glia 34, 178–189.

Toris, C.B., Zhan, G.L., Wang, Y.L., Zhao, J., McLaughlin, M.A., Camras, C.B., Yablonski, M.E., 2000. Aqueous humor dynamics in monkeys with laser-induced glaucoma. J. Ocul. Pharmacol. Ther. 16, 19–27.

Toris, C.B., Zhan, G.L., McLaughlin, M.A., 2003. Effects of brinzolamide on aqueous humor dynamics in monkeys and rabbits. J. Ocul. Pharmacol. Ther. 19, 397–404.

Tuulonen, A., Airaksinen, P.J., 1991. Initial glaucomatous optic disk and retinal nerve fiber layer abnormalities and their progression. Am. J. Ophthalmol. 111, 485–490.

Ueda, J., Sawaguchi, S., Hanyu, T., Yaoeda, K., Fukuchi, T., Abe, H., Ozawa, H., 1998. Experimental glaucoma model in the rat induced by laser trabecular photocoagulation after an intracameral injection of India ink. Jpn. J. Ophthalmol. 42, 337–344.

Varela, H.J., Hernandez, M.R., 1997. Astrocyte responses in human optic nerve head with primary open-angle glaucoma. J. Glaucoma 6, 303–313.

Vorwerk, C.K., Lipton, S.A., Zurakowski, D., Hyman, B.T., Sabel, B.A., Dreyer, E.B., 1996. Chronic low-dose glutamate is toxic to retinal ganglion cells. Toxicity blocked by memantine. Invest. Ophthalmol. Vis. Sci. 37, 1618–1624.

Wax, M.B., Tezel, G., Kobayashi, S., Hernandez, M.R., 2000. Responses of different cell lines from ocular tissues to elevated hydrostatic pressure. Br. J. Ophthalmol. 84, 423–428.

Weber, A.J., Zelenak, D., 2001. Experimental glaucoma in the primate induced by latex microspheres. J. Neurosci. Methods 111, 39–48.

Weber, A.J., Kaufman, P.L., Hubbard, W.C., 1998. Morphology of single ganglion cells in the glaucomatous primate retina. Invest. Ophthalmol. Vis. Sci. 39, 2304–2320.

WoldeMussie, E., Ruiz, G., Wijono, M., Wheeler, L.A., 2001. Neuroprotection of retinal ganglion cells by brimonidine in rats with laser-induced chronic ocular hypertension. Invest. Ophthalmol. Vis. Sci. 42, 2849–2855.